

No. 226
May 1980

IMPROVEMENT OF BARGE TOWING : TRANSLATIONS OF SELECTED JAPANESE AND RUSSIAN TECHNICAL ARTICLES

Translated by Robert Latorre



THE DEPARTMENT OF NAVAL ARCHITECTURE AND MARINE ENGINEERING

THE UNIVERSITY OF MICHIGAN
COLLEGE OF ENGINEERING

No. 226
May 1980

IMPROVEMENT OF BARGE TOWING: TRANSLATIONS OF
SELECTED JAPANESE AND RUSSIAN TECHNICAL ARTICLES

Translated by
Robert Latorre



Department of Naval Architecture
and Marine Engineering
College of Engineering
The University of Michigan
Ann Arbor, Michigan 48109

PREFACE

In response to commercial demands of river, coastwise, trans-ocean, and offshore operations, numerous barge designs are being developed. One of the problem areas confronted by the barge designer is the towing performance of the barge. This includes the barge towing resistance and the barge course stability during hawser towing.

The towing performance affects the barge's operation, scheduling, and ultimately its commercial success in service. The economy of barge and other waterborn transport is becoming more attractive with rising fuel costs and this will cause more congestion on the waterways. This congestion makes the towed barge course stability a critical safety factor and the rising fuel costs require that the barge towing resistance be reduced as much as possible.

Various Japanese and Russian researchers have studied these problems. They have extended the classic work of Strandhagen, Schoenherr, and Kobayashi published in the 1950 SNAME Transactions to model the effects of the barge skegs and the towing bridle. Systematic barge model tests have been made to study the effects of various skeg designs on the course stability as well as to improve the barge hull resistance. The basic part of this work has not been translated and remains relatively inaccessible to the rest of the maritime community.

The papers included in this report present the results of experimental and theoretical investigations of barge towing performance. They deal with the resistance of simple hull forms, as well as the improvement of the towed barge course stability from various skeg designs, skeg locations, towrope length, and bridle length.

I am grateful for the corrections Dr. K. Saito, Osaka University, and Professor K. Kijima, Kyushu University, added to the Japanese translations and for the corrections Professor Kirill V. Rojdestvenski, Leningrad Shipbuilding Institute added to the Russian translation. I would like to thank Mrs. L. Powell for typing the manuscript.

Robert Latorre

CONTENTS

No		Page
B-I-1	"On the Improvement for Various Performances of Work Vessels" by S. Ando	4
B-I-2	"Some Studies on the Course Stability of Towed Ships Systems" by S. Inoue, K. Kijima, M. Murakami, K. Sakata, and S. Lim	20
B-I-3	"On the Course Stability of a Barge" by S. Inoue, K. Kijima, and M. Doi	30
B-I-4	"Experimental Study on the Course Stability of a Towed Barge" by M. Tanaka	38
B-I-5	"Analysis of the Spontaneous Yawing of Towed Ships" by E. B. Yuden and A. G. Mikovsky	47

ON THE IMPROVEMENT FOR VARIOUS PERFORMANCES OF WORK VESSELS¹

BY

S. ANDO²

ABSTRACT

As ocean development becomes active, construction work using various kinds of work vessels has been increasing. A series of tests were performed in order to improve the form of work vessels with rectangular cross sections. As a result of the experiments it was shown that the propulsive performance can be improved by using a beveled bottom at the stem and stern. The beveled bottom's effect on the vessel's seaworthiness and maneuverability was also investigated. The investigations described in this paper concern the propulsive performance, seaworthiness, for the design, construction, and operation of work vessels.

TRANSLATION³

1. INTRODUCTION

The development of Japan's national economy and industrial base calls for improving the efficient use of the ocean regions. There is a rapid increase in harbor civil engineering, large scale construction of deep water harbors, construction of break waters, and the building of sea beds. This is also accompanied by a boom in the construction of undersea cables, oil exploration, and the manufacture of large scale wave observation buoys and towers.

Since these various operations and construction work are done at sea, various types of work vessels play a major role. Consequently, these vessels are classified by their functions and fittings. Typical classifications include: dredging, landfill, support operations, construction, research, as well as inspection.

These vessels usually operate in the calm ocean and harbors so ocean navigation has not been considered as their main activity. Consequently, with the exception of

a few examples, there is a relatively small amount of data and investigations for improving their seakeeping, maneuvering and safety characteristics.

Nevertheless as ocean engineering gradually expands into deep water ocean regions, these various work vessels will increasingly be confronted with severe weather and ocean waves. In addition to this, the importance of work vessels in the ocean transport of equipment and supplies is widely recognized. This is because unlike land based transportation there are no weight or volume limitations. Consequently there is a tendency towards relatively large size work vessels, as well as the construction of larger numbers of work vessels. At this point it has become important to acquire the basic data necessary for investigating the safety characteristics, operational potential, and operational efficiency of each type of work vessel. This data is also useful in work vessel design and construction.

At the Ship Research Institute, Mitaka, Japan, experimental research is conducted in general ship form and performance improvement. At the institute, work vessels with rectangular cross sections were selected from raft and slab type vessels and used in experimental investigations. Systematic tank tests were then conducted to improve the propulsive, seakeeping, maneuvering, as well as the safety characteristics of the vessels. This was done in addition to acquiring data for the design and construction of this type of vessel.

As mentioned earlier, because of the importance of work vessels, this paper summarizes the design trends and various performance improvements for work vessels with rectangular cross sections. The following is a discussion of such vessels with rectangular cross section (hence-

¹Transactions of the WEST JAPAN SOCIETY OF NAVAL ARCHITECTS, No. 50, August, 1975, pp. 83-98.

²Ocean Engineering Development Division, Ship Research Institute

³Prepared by Robert Latorre, Dept. of Naval Architecture & Marine Engineering, The University of Michigan.

forth referred to as the box form) treating the propulsive performance, seakeeping and maneuverability based on the author's investigations.

2. PROPULSIVE PERFORMANCE

The resistance and propulsive efficiency are essential factors in deciding the propulsive performance of a ship form. However since work vessels are usually towed rather than self-propelled when moving to their work site, ocean navigation has not been considered as their major role. Consequently work vessel propulsive performance is taken as the total resistance.

The resistance generally refers to the total resistance which is usually classified into a frictional resistance component and a residual resistance component. With the box form, the form resistance due to the fore part of the vessel represents a major portion of the total resistance. Namely, the residual resistance coefficient (obtained by subtracting the Schoenherr's frictional coefficient from the ship's total resistance coefficient) is about 70% to 80% of the total resistance coefficient. In the case of the box form, this is because the trim by the bow causes an increase in the wave and eddy making phenomena.

Fig. 1 presents the results of the box form being towed at various Froude numbers $F_n (\sqrt{V/gL})$ in calm water. This figure shows the total resistance coefficient $r_T = (R_T / 1/2 \rho V^2 \nabla^{2/3})$, trim $1/2 (d_F - d_A) \times 100/L$, and sinkage $1/2 (d_F + d_A) \times 100/L$. As the vessel is towed water is pushed ahead of the bow so the trim by the bow and sinkage becomes larger as the Froude number increases. From Fig. 1 it can also be understood that the resistance increases is aggravated by the vessel's sinkage and its trim by the bow.

Consequently, in order to reduce the box form's resistance the vessel's bow and stern form were modified by cutting away some of the fullness. This resulted in improvements in resistance, sinkage and trim which are described below. The power estimation was also made for a self-propelled work vessel.

2.1 REDUCTION IN RESISTANCE

Simple modifications were made to the vessel's bow and stern by cutting away some material as illustrated in Fig. 2. This figure shows the beveled bottom and beveled side modifications.

i) Beveled Bottom Bow and Stern [1], [2]

The three types of beveled bottoms used in the bow are shown in the upper portion of Fig. 2. In case a) the bevel lines go through the intersection of the forward perpendicular and waterline and the bevel angle α_B is measured from the perpendicular. As shown in Fig. 3, there is a tendency for the resistance coefficient, trim and sinkage to decrease as the value of α_B increases.

This reduction in the resistance coefficient with α_B appears in the results for various L/B and B/d ratios in Fig. 4.

For the various cases shown in this figure there is a reduction in the resistance coefficient up to values of α_B near 60° . Conversely, a stern bevel has little effect on the resistance coefficient until the value of the stern bevel angle $\alpha_S = 60^\circ$ as shown in the middle graph of Fig. 4. This may be caused by the effect due to the wake fraction at the stern and base drag.

In case b) the bevel lines pass through a point defined by $\alpha_B = 50^\circ$. Here the plot of the results for the bevel angle θ_B have been omitted. However, the trends showed that the minimum values for the resistance coefficient, trim and sinkage were in the vicinity of $\theta_B = 22^\circ$. In case c) the bevel lines form a constant angle of $\theta_B = 20^\circ$.

The reduction of the total resistance coefficient with the amount of material removed at the F.P. (l_d) is shown in the bottom graph of Fig. 4. In this figure, up to $l_d = 50\%$ there is a large reduction in the resistance coefficient and for values of l_d larger than 50% there is only a slight reduction in the resistance coefficient.

From the above results a value of α around 70° is the best for making the bow and stern bottom bevel from the viewpoint of resistance trim and sinkage. However, since navigating the ocean is not the main activity of work vessels, from considerations of efficiently using the working area and loading cargo it is good to use a bevel angle $\alpha = 70^\circ$ taken at a point of 1/2 draft.

ii) Beveled Sided Bow and Stern [1], [2], [5]

Modifications of the bow and stern sides are accomplished by making simple miter cuts or circular cuts to develop the three designs shown in the bottom of Fig. 2. In this figure the side modification a) is made by starting at the point at the side determined by a taper with $\beta_B = 50^\circ$. The resistance coefficient relationship with the bevel angle β_B is shown in the upper graph of Fig. 5. In Fig. 5 the total resistance coefficient has its mini-

imum value when β_B is approximately $15\sim 20^\circ$. Also while the figures are not shown, there was almost no variation in the trim and sinkage when β_B was changed. Following these tests, the stern was modified in the same manner, and there was almost no variation in the resistance coefficient as indicated by the results in the middle graph of Fig. 5.

The radius (R) cut b) was reported by Ikebuchi of the Shipbuilding Research Center of Japan in the magazine Senpaku [5]. The results are shown in the bottom graph of Fig. 5. When the radius R becomes smaller this graph shows the drastic reduction in the resistance coefficient. When this radius becomes larger its effect on the reduction in the resistance coefficient becomes small. It is natural for the ogive cut c) that there is a reduction in the resistance coefficient when the radius of the ogive becomes larger.

From this discussion, a bow bevel angle $\beta_B = 15^\circ$ is the optimum angle for bow side bevel angle of work vessels.

iii) Various Form Modification Schemes [1], [2], [3]

It appears that the bow and stern of work vessels will be assembled using more complex configurations than the simple modifications previously discussed.

Therefore, Fig. 6 shows a comparison of the total resistance coefficients of box shaped vessels with four types of complex bow shapes. From the results shown in this figure, the spoon bow form (d) has the lower resistance coefficient in the low speed region while at higher speeds the bow form (c) has a lower resistance coefficient than the spoon bow (d).

It appears from these results that it is possible for such box shaped vessels to obtain good resistance performance using comparatively simple beveled bow forms instead of adopting more complex forms.

2.2 FLOW AROUND THE HULL

The hull form found superior in the systematic resistance test series is shown in Fig. 7. It is a 1/18th model of an oil drilling vessel and this model was used to investigate the flow around the vessel's sides and the wake at the stern.

i) Flow Around Bow and Sides [3]

In order to observe the flow, 40 mm long tufts were attached 10mm apart from the surface of bow's slanting part and the vessel's sides. The flow was then observed while towing.

The flow pattern along the vessel's side at four different model speeds is

shown in Fig.8 as well as Photo 1 [Photo 1 has been omitted because it does not reproduce well]. The flow pattern along the side near the free surface has the same form as the vessel's wave profile. The flow near the vessel's bottom is aligned with the direction of the main flow. It appears that the flow along the vessel side has extremely simple streamlines.

Although the figure is not shown, it was found that the flow does not pass around the vessel's sides unless the bevel angle of the bow is near 20° . If the angle is different the flow does not pass around the sides and this results in a complicated flow along the bottom of the vessel.

ii) Wake at Stern [3]

The stern flow velocity distribution was obtained by using a spherical five hole pitot tube to measure the flow in the x, y and z directions. The measurement points are shown in Fig. 9. This is a detail of the upper left hand portion of Fig. 7. The results are shown in Figs. 10 and 11 (In these Figures the dashed arrows in the β section represent the measurement without the skeg).

The flow velocity in the x-z direction shown in Fig. 10 follows closely the bevel of the stern. Although the flow velocity in the y-z direction in Fig. 11 is nearly perpendicular along the hull centerplane, in the vicinity of the vessel's sides there is a strong tendency for it to flow outward.

From the above it appears that the skeg exerts very little influence on the notched section in Fig. 7.

The wake fraction at the aft sections are shown in Figs. 12 and 13. Fig.12 shows that because the skeg is fitted at the notched section the wake fraction values are very small irrespective of the model speed and location of each section. However, the extent of the notched section's influence on the wake fraction is evident in Fig. 13, showing the wake fraction with and without the skeg fitted. Therefore, from the viewpoint of the vessel's resistance and maneuverability performance it is worthwhile to fit skegs to the notched section.

2.3 ESTIMATION OF SHAFT HORSEPOWER FOR SELF-PROPULSION OPERATION [3]

In this section a summary is presented of the oil drilling vessel's estimated speed when it is self propelled using the digging equipment's prime mover.

This vessel has a length of 70m, a width of 50m and a draft of 4.58m and is

fitted with a 5,000 P.S. digging equipment's prime mover. The study was made for twin screw, twin rudder vessels designated as MA and MB. The MA vessel is shown in Fig. 7 while the MB form is fitted with bow section (c) shown in the upper part of Fig. 6. The propellers had a MAU blade section, a diameter of 0.1787 m., and were not optimally designed for both hull forms. Their open water characteristics are shown in Fig. 14. Fig. 15 shows the self propulsion coefficients measured from the self-propulsion tests with out-board turning propeller. The propulsive efficiency in this figure is extremely low in the range of .40. This is because the propellers tested were not optimum designs for the hull forms. Nevertheless it is possible to attain a speed above 6 knots when using the 5,000 horsepower for propulsion as shown in Fig. 16.

From the above it appears feasible to use the work vessel's machinery for propulsion to enhance its economic and safety effectiveness.

3. SEAKEEPING PERFORMANCE

Since the various types of work vessel forms were evolved from raft type vessels the work vessel hull has a nearly rectangular cross and these vessels have a wide beam in comparison to their length.

Thus, work vessels have a relatively superior hull form in comparison with general cargo or fishing vessels in regards to response in waves and related safety characteristics. Here an investigation is presented concerning the work vessel's Bertin's N coefficient which appears in the regulations related to the ship motion restoring performance. This influences the freeboard due to the relative motion of the vessel and wave surface. It also is used in estimating accelerations required for the design of the crane jib and digging tower. An investigation of the vessel's response in waves is also discussed since there is a wide variation in the center of gravity and radius of gyration of work vessels in comparison with those of the typical ship hull. In addition to this study the following discussion summarizes the effect of modifying the bow and stern on the response of the vessel in waves.

3.1 BERTIN'S N COEFFICIENT FOR BOX FORM VESSELS [8]

Free rolling tests were made in calm water for a wide range of conditions varying the center of gravity and radius of gyration of the models. The models used were a floating crane, grab dredger and pump dredger which have nearly rectangular cross section form. The Bertin's N coefficients obtained in these tests are shown in Fig. 17. In this figure the black triangles

indicate the Bertin's N coefficient for a general cargo ship filled with bilge keels. The N coefficient of the rectangular cross section work vessels is an extremely large value which is about 2.5 times the value of the general cargo ship fitted with bilge keels. Although the figure is omitted, the effective wave slope coefficient (δ) in the roll synchronism conditions was determined from the responses obtained from the forced rolling moment in calm water and in waves. For work vessels with OG/d less than 4.0, the value of δ has an extremely small value, $\delta = 0.07 + 0.175 \text{ OG/d}$ in comparison with that of a general cargo vessel [10], $\delta = 0.73 + 0.60 \text{ OG/d}$, whose center of gravity is in the vicinity of its waterline.

From the above facts it can be said that as far as response in waves is concerned, the work vessel has a superior hull form.

3.2 VARIATION OF RELATIVE WATER LEVEL ALONG THE VESSEL SIDES AND VERTICAL ACCELERATION [8]

In order to investigate the amount of variation in the water level along the sides of work vessels, tests were made in head (longitudinal) and beam (transverse) waves and the variation in water level at L/10 from the A.P. and F.P. on both sides of the vessel hull. An example of the results is shown in Fig. 18.

The upper portion of Fig. 18 shows the amount of water level variation in head waves with $\text{OG/d} = 2.1$, $K_{yy}/L = 0.53$ and $L/B = 2.2$. As expected, this figure shows that the variation in water level is the same along the port and starboard sides, and that the wave height reaches a value of 75% of the draft when the wave height and length ratio is 1/75. In the beam waves, the windward water level variation is about 3 times that of the lee side with short waves whose length is less than double (4 times the beam). This is because the vessel's hull acts as a wave absorber. However, for long waves this wave absorbing effect of the vessel hull diminishes and the differences in the port and sides disappear.

A general investigation of the accelerations was made for the structural strength design of the crane jib or the tower used on the work vessel. The vertical accelerations were measured at a height 1.0L from the vessel bottom and 0.45L forward of the bow for the test conditions: $L/B = 2.2$, $B/d = 6.0$, $\text{OG/d} = 3.5$, $k_{yy}/L = 0.53$, $k_{xx}/B = 0.40$. The vertical acceleration response in head and beam waves is shown in Fig. 19. From this figure it can be seen that the values of vertical acceleration (solid line) are much larger than the vertical accelerations estimated from the heaving motion in head waves. This may

be due to the high location where the acceleration was measured. The solid line in this figure shows the acceleration value predicted from the pitching motion, taking the distance between the measurement point and the intersection of the center of buoyancy and waterline as its lever. Therefore for work vessels with a relatively high center of gravity the vertical accelerations can be estimated by considering the pitching motion of the vessel.

The vertical accelerations in beam waves can be approximately estimated from the heaving motion (dashed line). This is because the rolling motion has a second order effect on the heaving motion (the center of the rolling motion is in the neighborhood of 80% to 90% KG).

This same tendency can be seen when a load is hung from the crane jib. (denoted as load in Fig. 19)

3.3 EFFECT OF ROUNDING THE BILGE [7]

As far as rolling motions are concerned vessels with a rectangular cross section possess a large roll damping coefficient. However, the use of construction ropes and chains used in the work vessel service requires adopting a bilge radius. Therefore, forced roll oscillation tests were conducted in calm water using two dimensional rectangular forms and gradually increasing the radius of the bilge at the vessel bottom.

Assuming the equation of rolling motion is given by:

$$(J_{\phi\phi} + A_{\phi\phi})\ddot{\phi} + B_{\phi\phi}\dot{\phi} + W \cdot GM = M_{\phi e}$$

Fig.20 shows the following values

$$(J_{\phi\phi} + A_{\phi\phi}) / \rho VB^2, \quad B_{\phi\phi} \cdot \sqrt{B/2g} / \rho VB^2$$

versus the bilge radius (r).

From this figure for the values of $r/B < 0.08$ there appears almost no variation in the virtual moment of inertia, while up to values of $r/B = 0.04$ there is a drastic reduction in the roll damping moment. This indicates that from the viewpoint of rolling motion it is advantageous to adopt a small bilge radius.

3.4 EFFECT OF CENTER OF GRAVITY AND RADIUS OF GYRATION ON ROLLING MOTION.

To estimate the rolling motion performance of various work vessels, wave tests were conducted with the vessel length, beam, draft, center of gravity as well as radius of gyration being systematically varied. In head waves the pitching motion is small as long as the wave length is below 0.8 times the vessel length which

is the same for typical ship hull forms. While for longer wave lengths at the maximum pitching values, the angle of pitching at its synchronism condition is 1.2 times the maximum wave slope value. The heaving motion has the same value as the wave height.

In beam seas, neglecting special situations, the maximum roll angle in its synchronism condition is 3 to 4 times the maximum wave height which is larger than the heaving motion measured in head waves.

From the above it is concluded that the major problem of the work vessel response in waves is its rolling motion.

The response performance of a model with $L/B = 2.2$, $B/d = 10.0$ is shown in Fig.21 illustrating the effects from changing the center of gravity and radius of gyration. Changes in the center of gravity have a larger effect on the rolling motion than changes in the radius of gyration. There is a tendency to reduce the roll angle when the center of gravity is raised because it appears that when the center of gravity is raised the wave length correspondingly becomes longer and the wave slope angle becomes smaller in conditions of constant wave height.

The usual method for estimating approximately the magnitude of the motions in waves is done by using the Ordinary Strip Method (OSM) with the hydrodynamic forces on the two dimensional section determined by the Ursell-Tasai analysis or the source distribution method. With the exception of roll damping the theoretically determined hydrodynamic forces and wave excited forces are in agreement with the experimental values. The experimentally obtained damping coefficient is assumed to be divided into wave damping and viscous damping components. In addition the experimentally obtained damping moment A_R and the theoretical damping moment A_{RO} obtained from the Ursell-Tasai or source distribution method are assumed to be related by

$$A_R = \sqrt{A_{RO} + b\xi^n} / d, \quad B_{\phi\phi} = \rho g^2 (A_R \cdot B/2)^2 / \omega^3$$

where the constants b and n were shown by Okawa [9] to give the best approximation when $b=0.70$ and $n=2.5$.

3.5 EFFECT OF BEVELED BOW AND STERN

The effectiveness of beveled bottom and sides in improving the propulsive performance was discussed in section 2.

This led to towing tank tests which investigated the effects on the responses in waves from beveling the box form vessel's bow and stern. These experiments were made in head and beam waves while maintaining the following parameters constant:

$L=1.80$ m, $L/B=3.0$, $B/d=5.0$, $KG/d=1.67$
 $K_{xx}/B=0.35$, $K_{yy}/L=3.0$. The bottom bevel
modifications (b) and (e) as well as the
mitered beveled side modification (a)
shown in Fig.2 were tested.

i) The influence of the bow bevel angle θ_B on the vessel motions is shown in Fig. 22. From this figure it appears that the pitching and heaving motions in head waves and the heaving and swaying motions in beam waves are nearly unaffected by the bevel angle θ_B .

However, the rolling and surging motions appear to be strongly influenced by the value of θ_B . Regarding the rolling motion, it appears that when the bevel angle increases above $\theta_B=20^\circ$ there is a tendency for the roll angles to increase. As for the surge motion, it appears that as the resistance becomes smaller as θ_B increases there is an increase in the surge motion.

ii) The influence of the bow side bevel angle β_B on the motions is shown in Fig.23. In this figure it appears that the miter angle β_B has a small influence on the motions in head waves. Namely near the value $\beta_B=20^\circ$ there is a reduction in the motion. On the other hand, the value of β_B has almost no influence on the the motions in beam waves.

iii) The influence of l_d/d on the motions is shown in Fig.24. In these tests the bow bevel angle was maintained at $\theta_B=20^\circ$

The influence of l_d/d on the motions is the same as for θ_B namely it affects only the rolling and surging motions and there appears to be no effect on the other motions. Considering the influence of l_d/d on the rolling and surging motions, they are reduced when the value of l_d/d is small.

From the above results it can be concluded that a bow form having a bevel angle near $\theta_B=20^\circ$ with a spacing of $l_d/d = 0.5$ and a side miter angle $\beta_B=15^\circ$ which is superior from standpoints of resistance trim and sinkage does not result in poor responses in waves in comparison to those of rectangular form.

4. STEERING PERFORMANCE [1],[3]

Since navigation has not been a major role of work vessels their steering performance has not been considered a major problem. However, from considerations of safety and economy, it is expected in the

future the power used for the operations will be utilized for the vessel's propulsion and it is therefore necessary to investigate the vessel's steering performance.

Initially oblique towing and turning tests were made with models having rectangular cross sections. These models had $B/d=10.0$ and length to beam L/B ratios of 1.0, 1.5, 2.25 and 3.0. The three force components (drag force X , normal force Y , and moment around the center of flotation M) were measured. The results indicated that the trends in the forces for the $L/B=1.0$ model were extremely different than those of the other L/B ratios. (This figure is omitted). The lift force coefficient C_N obtained from the test data of the three forces is shown in Fig.25. The trends in this figure for $L/B=1.0$ lift forces is shown in Fig.25. The trends in this figure for $L/B=1.0$ lift coefficient are extremely different in comparison with the other L/B ratios. The lift force at the beginning of the turn for the $L/B=1.0$ corresponds to the lift force in the opposite direction for L/B ratios larger than 1.5. In these experiments neither propellers nor rudders were fitted. It can be anticipated that when they are fitted the vessel will run in a straight direction in similar situations since the rudder angle used in turning does not result in a large turning force.

Next the self-propelled turning tests were made with these rectangular form work vessels with twin screws and rudders. The results of these tests are presented in the form of non-dimensional turning angle velocity (vessel length/turning radius), maximum advance, maximum transfer, as well as turning radius indicated by the solid lines in Figs. 26 and 27. It can be understood from this figure that below values of $L/B=1.0$ turning is difficult.

Following these tests, self propelled turning tests were conducted using a beveled bow whose angle is 22° fitted to the previously described work vessel models. The results of these tests are indicated by the dashed lines in Fig.26 and 27. It can be understood from these figures that the beveled bow causes a large improvement in the turning performance and there is almost no reduction in the course keeping performance. However, for L/B ratios less than 1.0 adopting a beveled bow does not result in an improved turning performance as with the rectangular form

The results of an investigation of the effect of using the beveled bow modification (b) in Fig.2 on the turning performance is shown in Fig. 28. From these results good turning performance is obtained, especially when the bevel angle

$\theta_B=22^\circ$ and the non dimensional angular turning velocity becomes large. Namely, at this value the turning radius is small. At the same time as far as obstacle avoidance is concerned it is important to have a maximum advance and a maximum transfer while at $\theta_B=22^\circ$ these values are minimum.

From the above it is understood that the beveled bottom is also able to change the turning performance.

5. CONCLUSION

The previous discussion has treated the main results obtained from systematic model tests of the resistance, seakeeping, and turning performance of work vessels with rectangular cross sections tested at the Ship Research Institute. The following is an enumeration of the details for the improvement of work vessels by the synthesis of the experimental results including the experimental results not included in this presentation.

i) For the work vessel which has a good resistance performance without making major changes to the hull form it is good to bevel the bow and stern using $\theta_B=20^\circ$ measured from a point half the full load draft and adopting a mitered side with an angle of $\beta=15^\circ$. Also, if possible it is good to round the bevel ends. If it is not possible to use mitered sides, then it is good to use an $R/B=0.05$ radius. It is also worthwhile in case of self propulsion to use a beveled stern which makes an angle $\theta=20^\circ$ from the bottom to 80% the full load draft.

It appears there remains further possibility to improve the work vessel hull form. After many years of experience, research, and development, the apparent ideal hull form for very large full ship forms ($C_B=0.81$, $L/B=5.8$, $B/d=3.1$)

was arrived at which has a total resistance coefficient around $0.02=0.04$ at a Froude number near 0.2. In comparison a rectangular hull form of the same proportions with the previously described beveled bow and stern has a total resistance coefficient of 0.04-0.06.

ii) When the beveled bow and stern are adopted (as described earlier) to improve the resistance characteristics, they do not have a bad influence on the vessel motions in waves compared to the response of the rectangular hull form.

Because there are many occasions when mooring or working cables are used on the work vessels it is necessary to round the bow, stern and bilge in order to prevent the cables from breaking. For this requirement the previously recommended radius is adequate. In order not to re-

duce the roll damping force by rounding the bottom at the bilge, it is advisable not to make it round but use a radius within 1/100th of the beam ($R/B=0.01$).

iii) A difficult point in existing work vessels with rectangular cross sections is their turning performance. For the large full ship ($C_B=0.81$, $L/B=5.5$, $B/d=2.6$) at a 40° rudder angle the non-dimensional angular turning velocity is 1.0 while in comparison, the previously described optimum hull form has a non-dimensional angular turning velocity of 0.5 to 0.6.

The major factor influencing the work vessel's turning performance is its rectangular cross section. The rectangular cross section is different from the usual ship's midship section featuring a bilge radius.

In addition, it is not anticipated that adopting beveled bottom or sides on vessels with the same length and width ($L/B=1.0$) will improve their turning performance.

Finally the author is deeply grateful to Dr. T. Ito director of the Ship Propulsion Division of the Ship Research Institute and Dr. I. Ueno, director of the Ocean Engineering Development Division for their guidance and direction throughout this study. The author is thankful to Mr. Okawa for his planning of the investigation and discussion of the results. Thanks are also given to Mr. Takai and Mr. Yago for their cooperation in carrying out the experiments.

NOMENCLATURE

L	vessel length
B	vessel beam
d	vessel draft
d_F	forward draft
d_A	aft draft
∇	volumetric displacement
W	displacement
V	vessel speed
F _n	Froude number
R_T	total resistance
r_T	total resistance coefficient
α_B	bow bevel angle [Fig.2]
α_S	stern bevel angle [Fig.2]
β	bow bevel angle [Fig.2]
ℓ_d	bow cutting height [Fig2]
β_B	mitered bow angle
β_S	mitered stern angle
\sqrt{x}	flow velocity in X directions in stern
\sqrt{y}	flow velocity in Y direction in stern

REFERENCES

V_z flow velocity in Z direction in stern
 V_m model towing velocity
 J advance coefficient
 K_T thrust coefficient
 K_Q torque coefficient
 η_o Propeller open water efficiency
 η Propulsive efficiency
 η_R relative rotative efficiency
 $1-t$ thrust deduction factor
 DHP delivered horse power
 X_a surging amplitude
 Y_a swaying amplitude
 Z_a heaving amplitude

 θ_a pitching amplitude
 ϕ_a rolling amplitude
 λ wave length
 k wave number ($2\pi/\lambda$)
 N Bertin's damping coefficient
 ω circular frequency
 $A_{\phi\phi}$ added mass moment of inertia
 $B_{\phi\phi}$ damping moment
 $J_{\phi\phi}$ mass moment of inertia
 A_R non-dimensional damping moment
 ξ_d non-dimensional circular frequency ($\omega^2 d/g$)
 η_a water level amplitude on vessel sides
 \ddot{Z}_a vertical accelerations
 C_N lift coefficient
 β drift angle
 δ rudder angle
 r' non-dimensional angular velocity

 D_A maximum advance
 T_R maximum transfer
 D_T turning circle
 \overline{OG} distance between center of gravity and waterline
 \overline{KG} distance between center of gravity and bottom
 \overline{GM} distance between center of gravity and bottom
 K_{xx} radius of gyration for rolling
 K_{yy} radius of gyration for pitching
 C_B block coefficient
 ζ_a wave amplitude
 ρ water density
 g acceleration of gravity

(Propulsion and Maneuverability Performance)

1. Ando, S., "Some Ideas on the Improvement of Work Vessel Performances" SAGYOSEN, No 94, July, 1974 (In Japanese)
2. Ando, S., "On the resistance of the box form work vessel," Bulletin of the Society of Naval Architects of Japan, No. 518, August 1972 (In Japanese)
3. Ando, S., et. al. "The Resistance and Maneuverability Performances of the Boxshaped Work Vessel," (Nos.1,2,3, and 4) Summary of the Ship Research Institute Meeting No. 16,18,20,and 22) (In Japanese)
4. Hay, A.D., "Resistance of Barge Forms," The Marine Engineer and Naval Architect, Sept., 1949
5. Ikebuchi, Y., "Resistance Tests for Boxshaped Floating Vessels," SENPAKU, Vol. 47, Nov., 1974 (In Japanese)

(Seakeeping)

6. Ando, S., et. al. "Experiments of Boxshaped Vessels in Waves" (1st, 2nd) Summary for the Ship Research Institute Meeting (20th and 22nd) (In Japanese)
7. Ando, S., et.al. "Motions of Boxshaped Work Vessels in Waves (1,2,3) Summary for the Ship Research Institute Meeting (20 and 22) (In Japanese)
8. Ando, S., and Takai, R., "Motions of Work Vessels in Waves," Summary for the SRI Meeting (24) 1974. (In Japanese)
9. Okawa, Y., "On the Hydrodynamic and Wave Exciting Forces on Box Form Vessels in Beam Seas," Unpublished, May, 1975
10. Motora, S., Dynamics for Ship Motions, KYORITSU-SYPEBU Ltd. 1967.

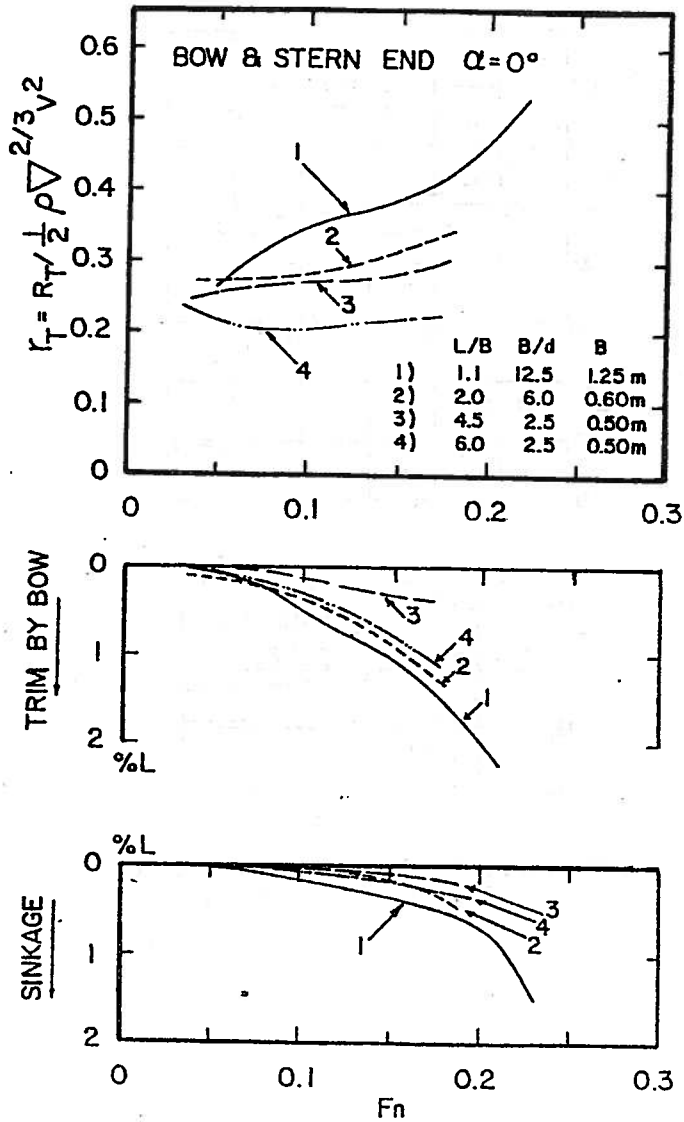


FIG. 1 Total Resistance Coefficient, Trim, and Sinkage of Box Shaped Vessels

FIG. 2 Side and Bottom Bevel

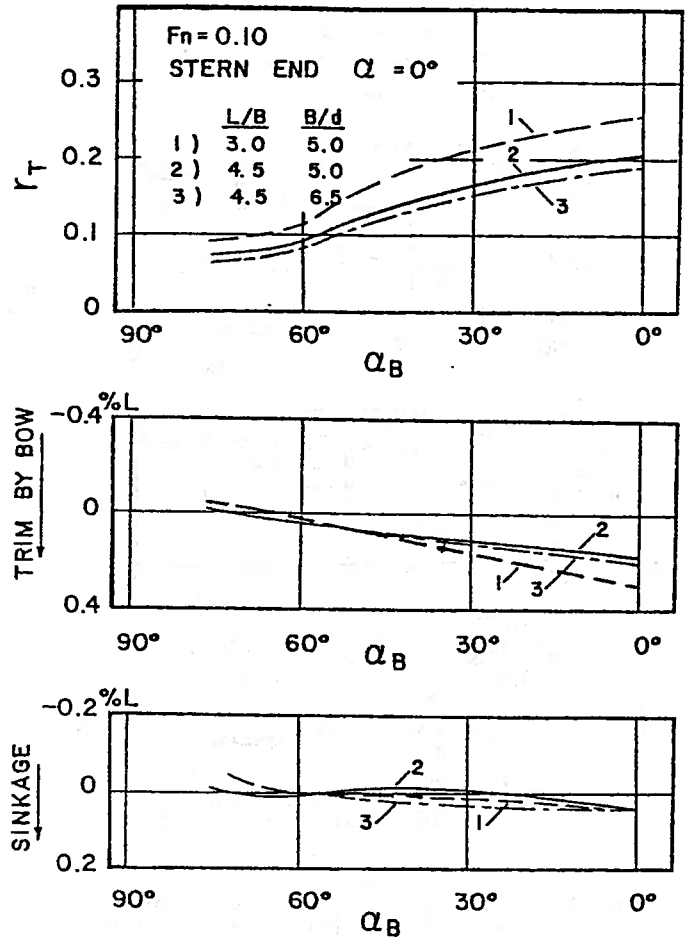
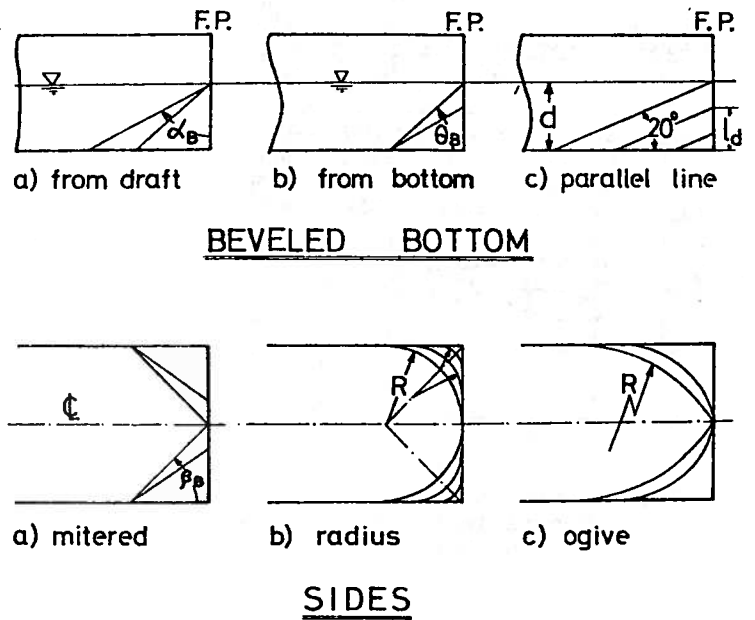


FIG. 3 Effect of Bow Bevel, α_B , on Total Resistance Coeff., Trim and Sinkage

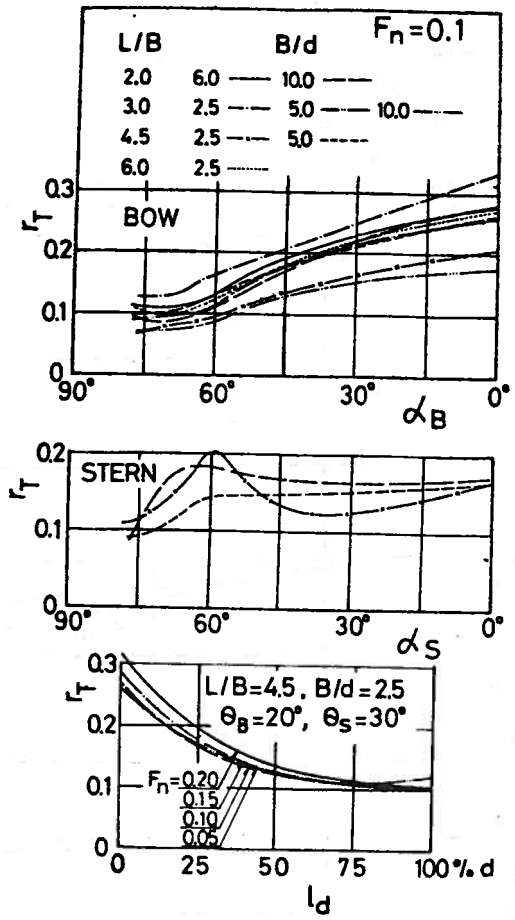


FIG. 4 Variation in Total Resistance Coefficient with Bottom Bevel

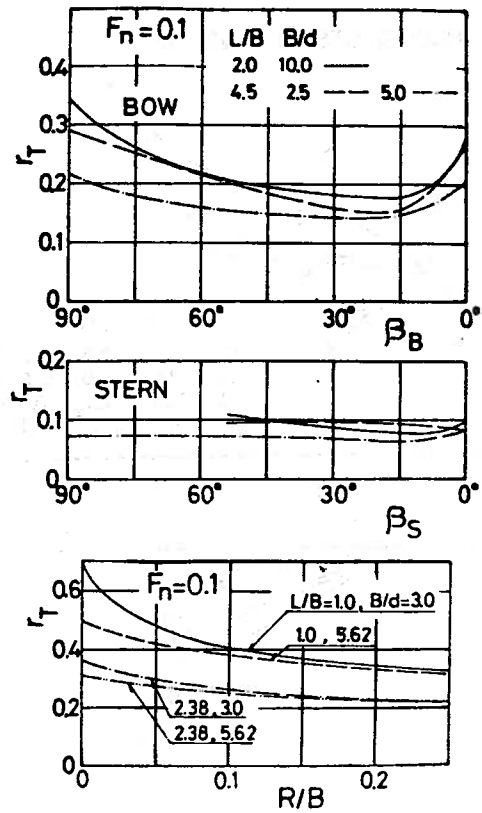


FIG. 5 Variation in Total Resistance Coefficient with Side Bevel

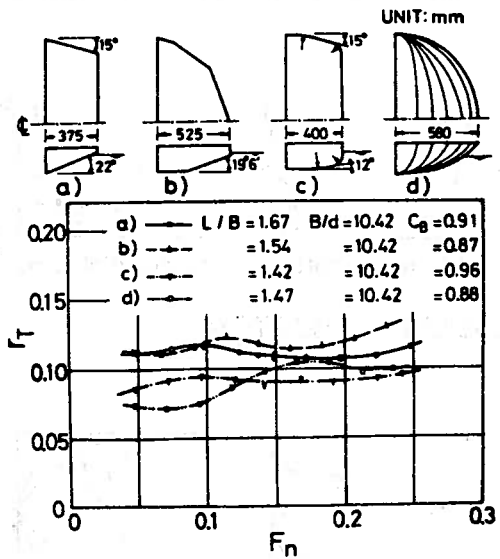


FIG. 6 Comparison of Total Resistance Coefficients of Different Complex Bow Forms

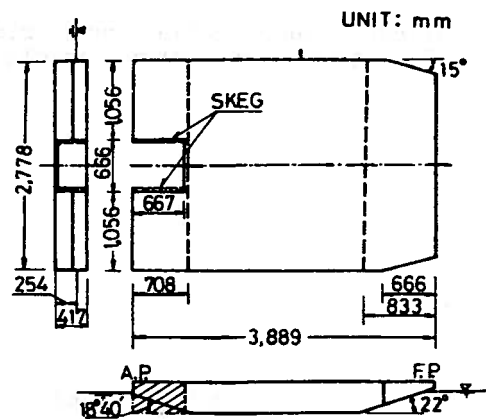


FIG. 7 Plan of Oil Drilling Vessel's Hull Form

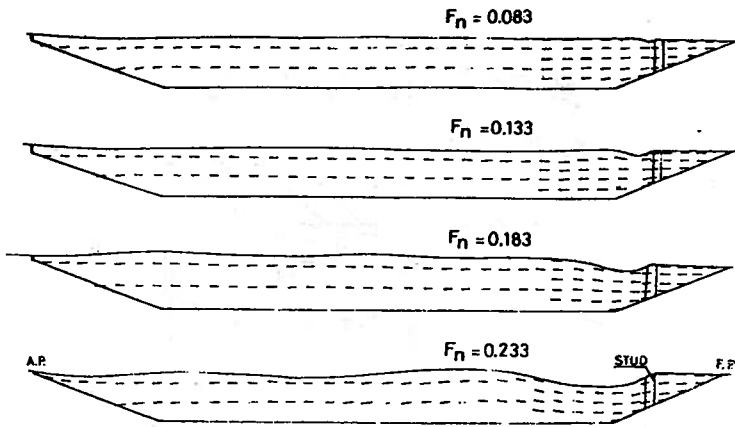


FIG. 8 Flow Pattern Along Vessel Side

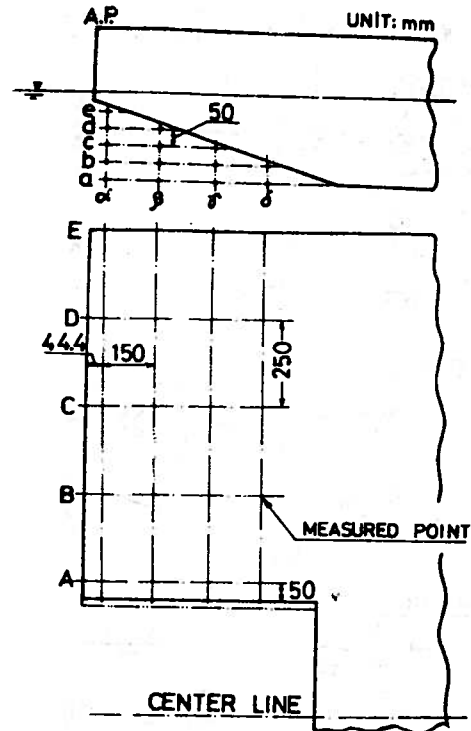


FIG. 9 Location of Flow Measurement on Vessel's Stern

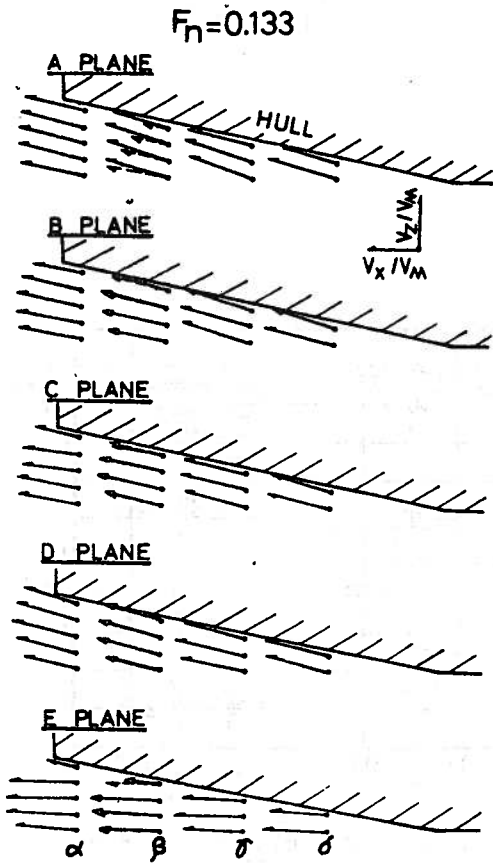


FIG. 10 Velocity in the x-z Direction on Vessel's Stern

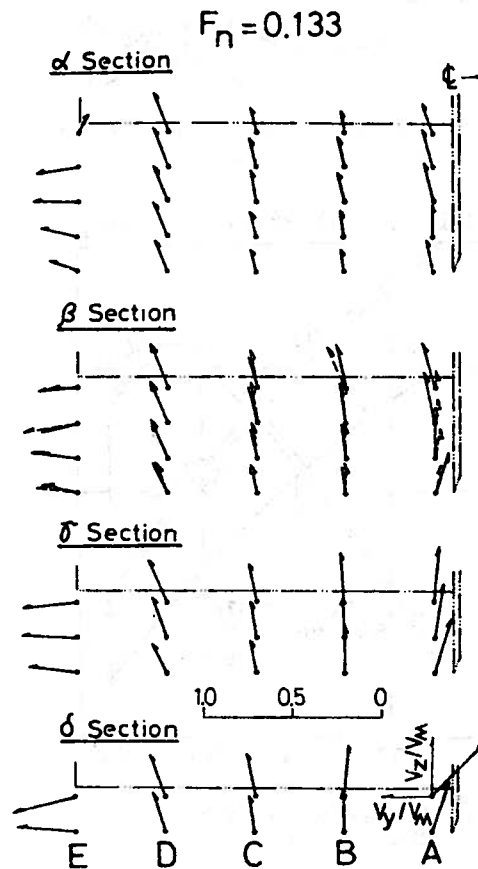


FIG. 11 Velocity in the y-z Direction on Vessel's Stern

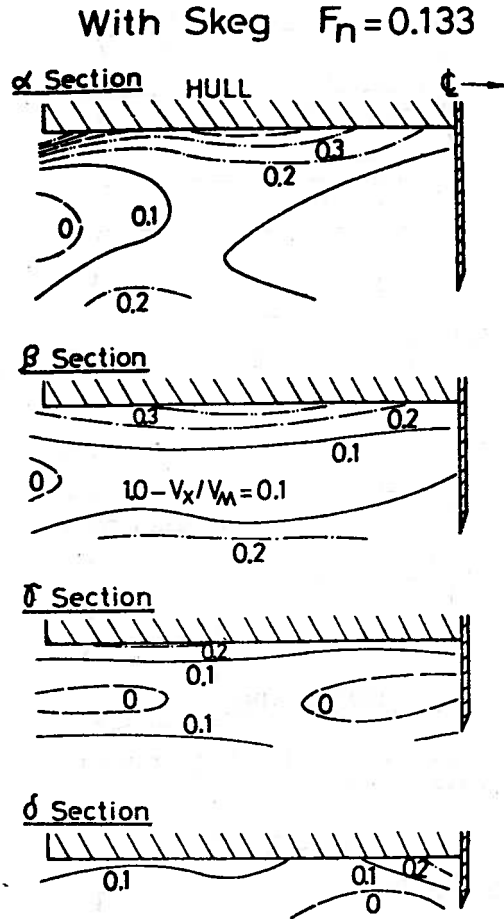


FIG. 12 Wake Fraction along various Stern Sections

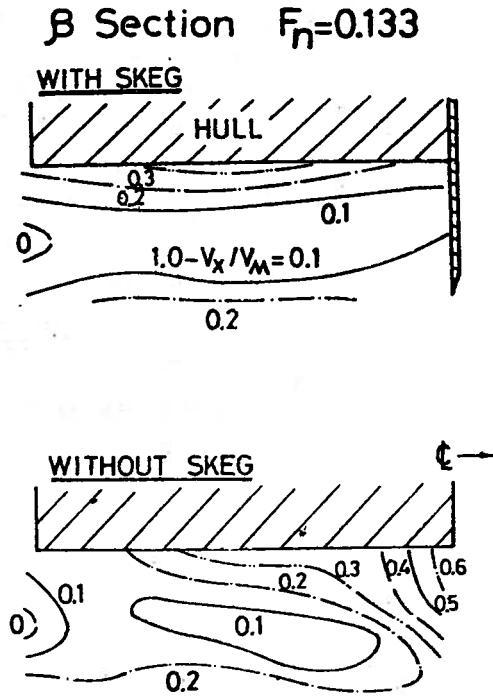


FIG. 13 Comparison of Stern Wake Fraction with and without Skegs Installed

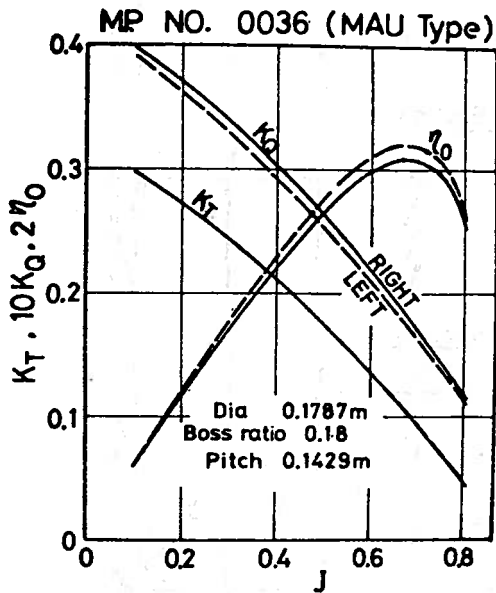


FIG. 14 Propeller Open Water Characteristics

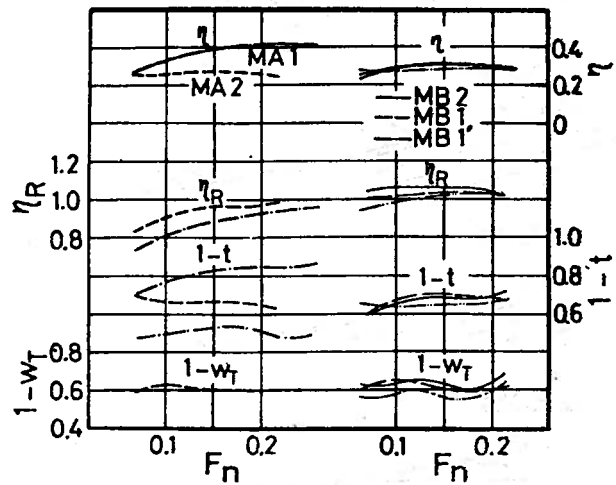


Fig. 15 Self Propulsion Coefficients for each Hull Form

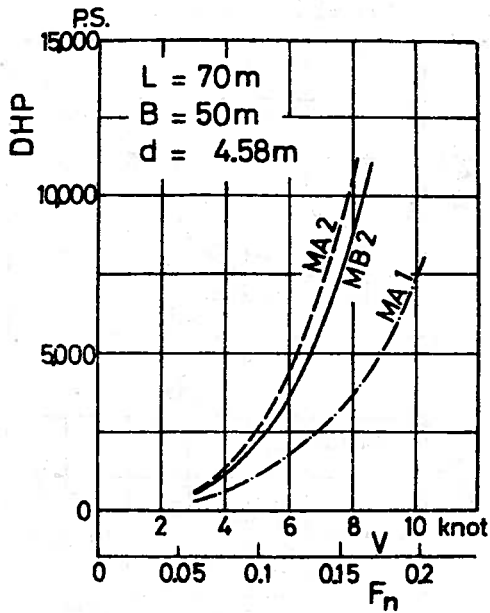


FIG. 16 Estimated Required Power

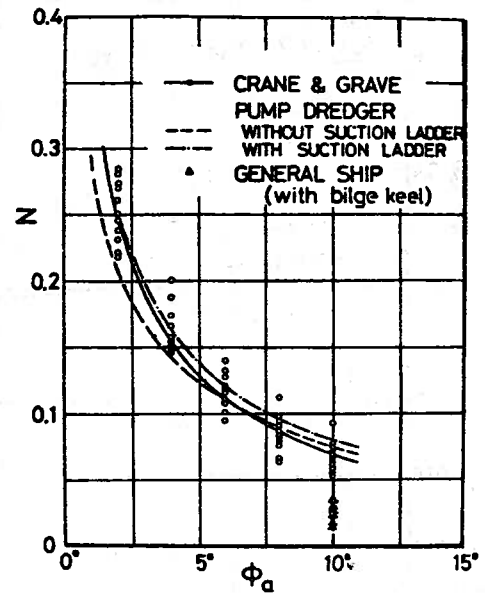


FIG. 17 BERTIN'S N Coefficient for Work Vessels

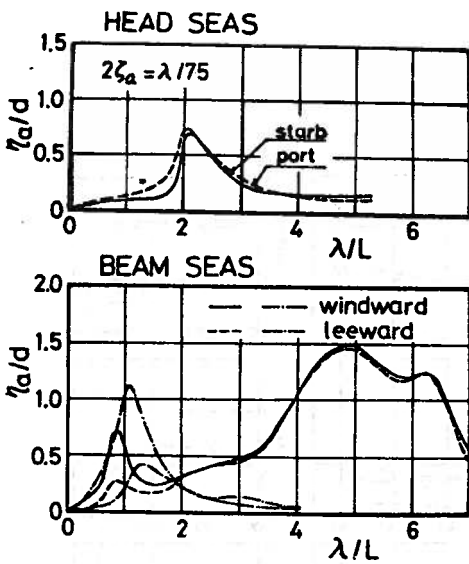


FIG. 18 Variation of Water Level along Sides of Work Vessels

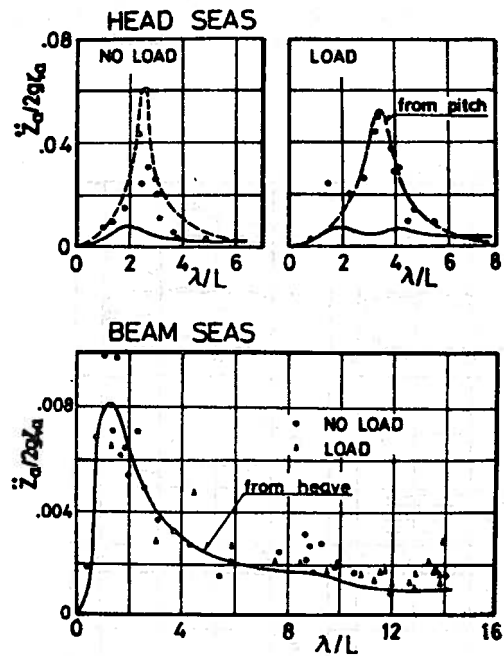


FIG. 19 Vertical Acceleration of Floating Crane with and without a suspended weight

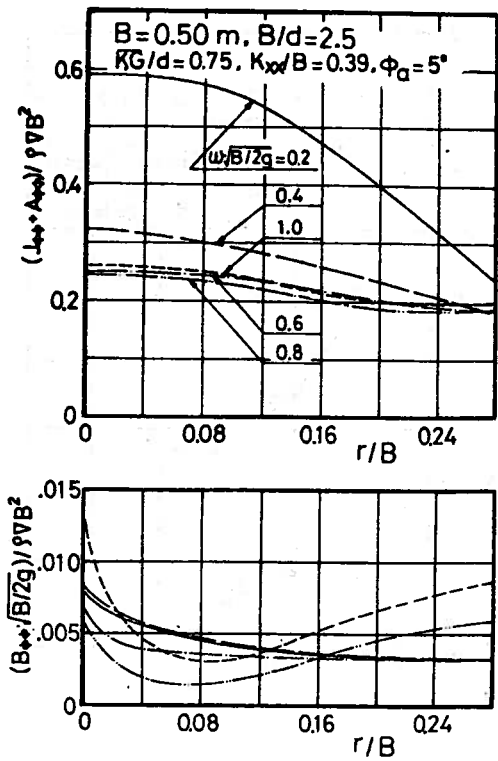


FIG. 20 Influence of Bilge Radius on the Virtual Moment of Inertia and the Roll Damping Moment

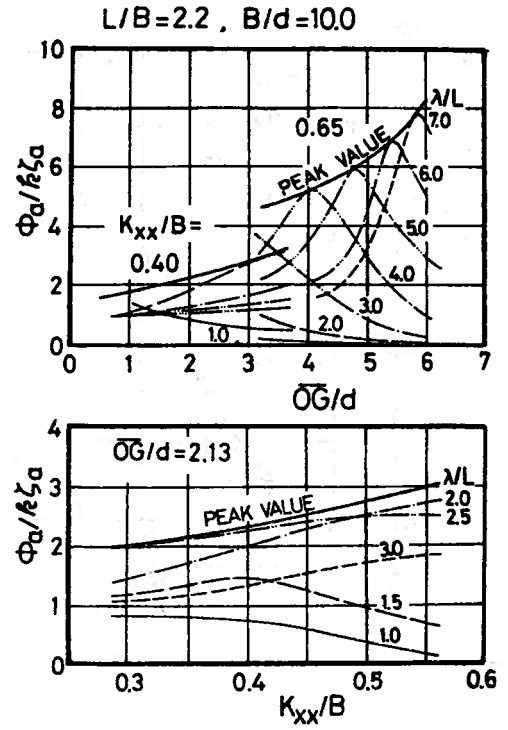


FIG. 21 Effect of the Center of Gravity and Radius of Gyration on the Vessel's Rolling Motion

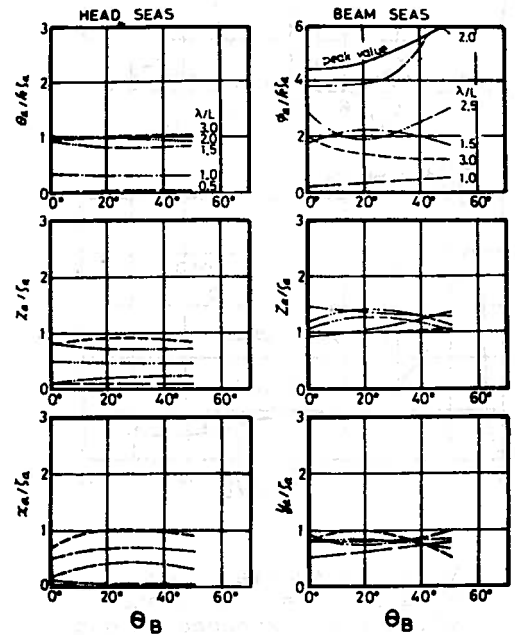


FIG. 22 Effect of Bottom Bevel on the Vessel's Motion

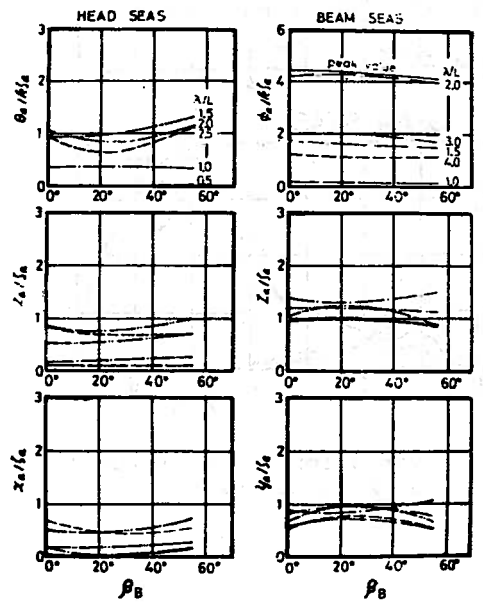


FIG. 23 Effect of Side Bevel on the Vessel's Motion

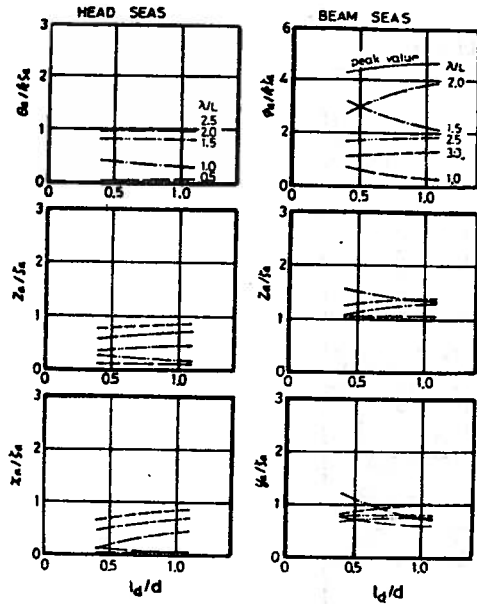


FIG. 24 Effect of Bevel Bottom Cut-Away on Vessel Motion

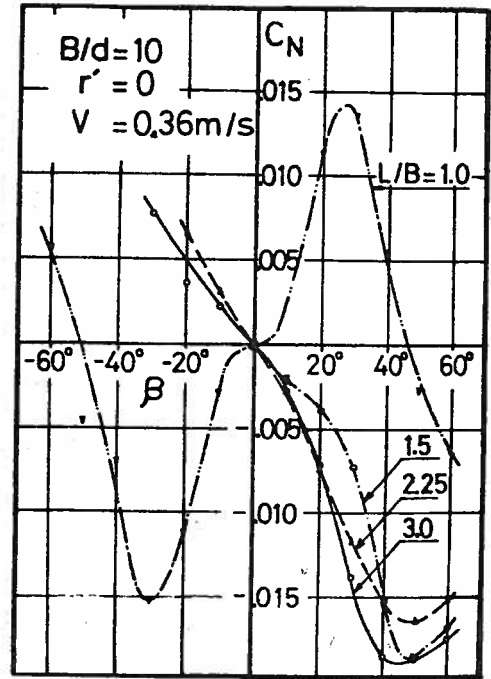


FIG. 25 C_N of Rectangular Form Vessels During Turning

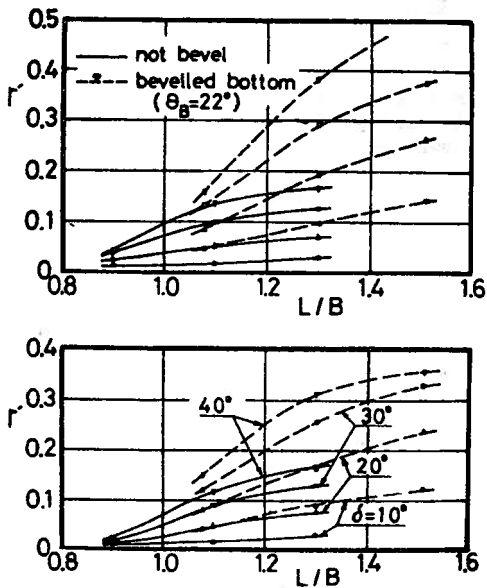


FIG. 26 Influence of L/B Ratio on Advance, Transfer, and Turning Radius

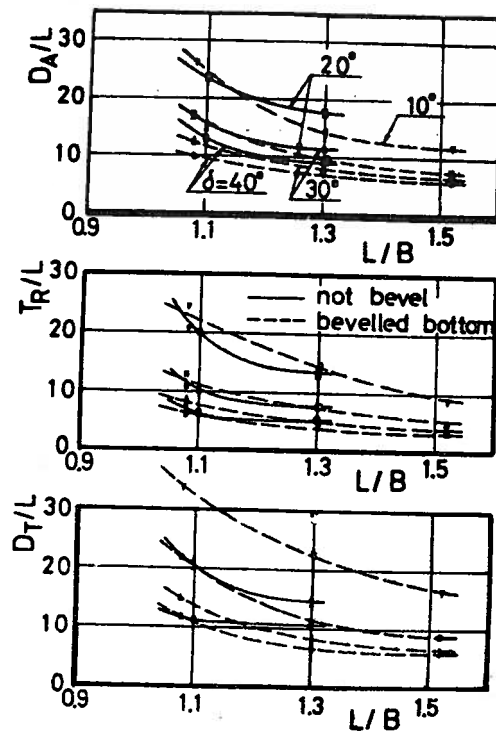


FIG. 27 Influence of Bow Bottom Bevel Angle on Turning Performance

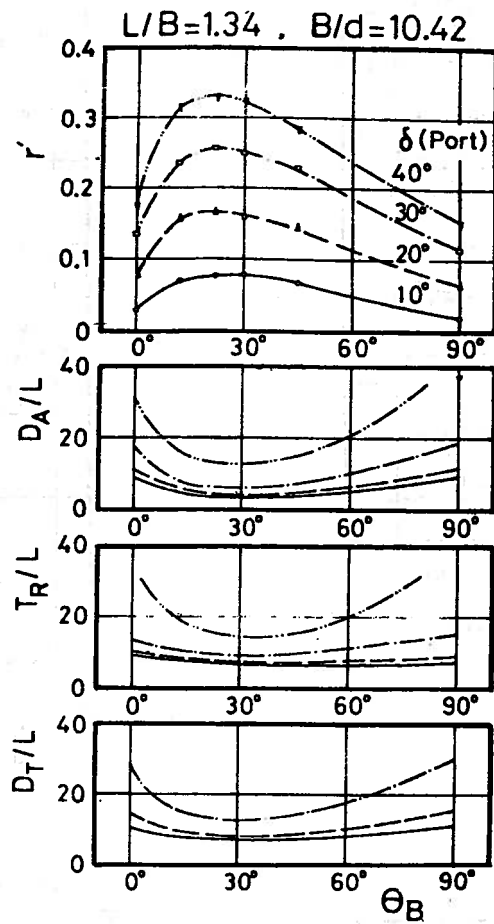


FIG. 28 Influence of Bow Bottom Bevel Angle on Vessel's Turning Performance

SOME STUDIES OF THE COURSE STABILITY OF TOWED SHIPS SYSTEMS¹

BY

S. INOUE²
K. KIJIMA²
M. MURAKAMI²
K. SAKATA³
S. LIM²

ABSTRACT

As we have discussed in this Journal (Nos. 42,43,44 and 46), the course stability for a towed ship system is influenced by the parameters: a) number of towed ships, b) fore- and aft-towing points, c) towing ropes' lengths, e) means of steering, f) course stability criterion of a ship g) radius of gyration, and h) resistance of towed ship. The effects for these parameters are as follows:

a) The larger the number of towed ships, the poorer the course stability is, and while stable towing of one towed ship is possible by adopting a suitable towing point and the tow rope length, it becomes impossible to tow more than two ships without steering.

b) The effect of aft-towing point is small, and in the case of forward towing point, it is better to place it away from the towed ships' center of gravity.

c) A longer tow rope provides more stable towing than shorter tow ropes.

d) The course stability of a towed ship system increases with the increase of a ship's course stability criterion, and this effect becomes smaller for two and more towed ships.

e) By means of steering, the course stability increases remarkably.

f) The course stability of same sized towed ship is better than the large towed ship in the case of the same parameters of each ship.

g) When the radius of gyration increases, the course stability grows worse, even for one towed ship and when the radius of gyration is greater than $0.50L$, it is impossible to have stable towing without steering.

h) As the resistance of the towed ship increases, we obtain stable towing of the towed ship system

When an unstable ship like a barge is towed, its course stability is very poor (described in d) and to obtain stable towing for towed ships such as barges, the course stability of the barge itself should be improved by utilizing skegs. In this paper, towing experiments for a single barge and tugboat and oblique test of the barge for the conditions shown in table 2, have been performed and the results are as follows:

1) When the skeg is fitted to the barge, because of the increment of Y' and the decrement of N' , course stability of the towed ship system improves very much, so that when the high lift skegs like the slotted flap skeg and the slotted flap with rotor skeg are fitted to the barge, it is not difficult for us to imagine that the course stability of this system improves.

2) For the towing test of towed ships system, due to the effect of towed ship size (see Ref. 1,2,3,4), it is not suitable to test in towing tanks with narrow breadth. In other words, it is necessary that they be towed by a tugboat in a wide surface area performance facility.

TRANSLATION⁴

1. Introduction

The authors have up to now made numerous theoretical studies concerning the towing of towed vessels. The course stabi-

¹TRANSACTIONS OF THE WEST-JAPAN SOCIETY OF NAVAL ARCHITECTS, No. 50, August 1975, pp. 65-74

²Department of Naval Architecture, Faculty of Engineering, Kyushu University.

³Matsukura Kaigi Co., Ltd.

⁴Prepared by R. Latorre, Department of Naval Architecture and Marine Engineering University of Michigan.

lity of a towed vessel is determined by assuming the towing rope as a weightless string which only transmits the tension force. If the towed vessel can be considered stable with the above assumption, then it not necessary to be concerned with the mass and elasticity of the towrope influencing the course stability. [1],[2],[3],[4].

When unstable vessels such as barges are considered as a towed ship system, their course stability performance is extremely poor. This paper discusses the course stability of a towed barge with skegs fitted to both sides of the stern in order to improve its course stability performance. This is examined by towing experiments as well as oblique towing tests which are presented with a discussion of the towing ship-towed vessel system experiments.

II. FACTORS INFLUENCING THE COURSE STABILITY

In the towing problem, the following factors are influential:

a) number of towed vessels, b) size of towing vessel and towed vessels, c) length of the towing rope, d) location of towing point (forward and aft), e) the quality of each vessel's course stability performance, f) the size of the radius of gyration with respect to the center of gravity of each vessel, g) the increase and decrease of the tension force which can be said to represent the increase and decrease of vessel's resistance, and h) steering.

In (a) when the number of vessels increase the towing becomes unstable [1],[2]. In (b) when the towed vessel becomes larger, the course stability becomes poorer as shown in Fig.2.

In (c) when the towrope becomes longer the course stability improves, but it is not desirable for it to become too long from the viewpoint of turning performance and navigation.

In (d) it is better if the forward towing point extends a distance ahead of the bow. An example of this is the generally used bridle system. Also, it will be best to locate the center of gravity behind the towing point.

In (e) the course stability performance of each vessel can be described by:

$$\Delta = Y'_\beta N'_r - (m_x Y'_r) \cdot N'$$

(where $Y' \dots Y'_r \dots$ are called the static and rotary derivatives respectively which can be experimentally as well as theoretically determined) When Δ is large the vessel's course stability performance is good, and when $\Delta < 0$ the vessel becomes course unstable, Fitting skegs causes a large increase in

the value of Δ . The skeg derivatives are denoted by L'_β and L'_r . The derivatives of the vessel with skegs are denoted by a bar — . The following relations are obtained when the skegs are fitted in the stern:

$$\bar{Y}'_\beta = Y'_\beta + L'_\beta$$

$$\bar{N}'_\beta = N'_\beta - b' L'_\beta$$

$$\bar{Y}'_r = Y'_r + L'_r$$

$$\bar{N}'_r = N'_r + b' L'_r$$

Here b' is the ratio of the distance between the skeg's center of pressure and the vessel's center of gravity to the length of the ship. It is possible to write:

$$L'_r \doteq b' L'_\beta$$

Basically the derivatives L'_β and L'_r are associated with the lift L generated by the skegs which causes a corresponding increase in Δ and an improvement in the course stability performance. Consequently skegs which cause increases in L'_β or high lift may be preferable. With a larger value of Δ , it becomes possible to use shorter towrope lengths and to locate the towing point closer to the vessel's center of gravity.

In (f) when the radius of gyration becomes larger, the vessel becomes course unstable. An example is shown in Figs. 3 and 4.

In (g) the increase of resistance causes an improvement of course stability. Consequently, not only from this point of view, but also from a large improvement in Δ (discussed in (e)) it is recommended to fit skegs.

In (h) when the vessel is steered in proportion to its course, its course stability is extremely good, and there is a remarkable improvement in the course stability of the towing boat itself.

III. EQUATION OF MOTION FOR N NUMBER OF TOWED BARGES FITTED WITH BRIDLES

Fig.1 shows the $i-1$ to $i+1$ towed vessels of a towed barge system. Here we consider the equilibrium conditions for forces by making use of the notation used in previous four articles [1],[2],[3],[4].

From Fig.1 it can be seen that:

$$\text{Cos} \sigma_{li} = B_i / 2\bar{\ell}_i, \quad \text{sin} \sigma_{li} = f_{2i} / \bar{\ell}_i$$

In the case when $\epsilon_i < \pi/2 - \sigma_{li}$ from equilibrium of forces:

$$T_{1i}' \cos\left(\frac{\pi}{2} - \sigma_{1i}\right) + T_{2i}' \cos\left(\frac{\pi}{2} - \sigma_{2i}\right) = T_i' \cos \epsilon_i \quad (2)$$

$$T_{1i}' \sin\left(\frac{\pi}{2} - \sigma_{1i}\right) + T_{2i}' \sin\left(\frac{\pi}{2} - \sigma_{2i}\right) = T_i' \sin \epsilon_i$$

Now assuming that ϵ_i is very small it is possible to make the approximation:

$$\cos \epsilon_i \doteq 1, \sin \epsilon_i \doteq \epsilon_i \text{ and } \sigma_{1i} \doteq \sigma_{2i}$$

Then from (2) the following expression is written:

$$T_{1i}' + T_{2i}' \doteq T_i' \frac{\tilde{\ell}_i}{f_{2i}} \quad (2)'$$

$$T_{1i}' - T_{2i}' \doteq T_i' \frac{2\tilde{\ell}_i}{B_i} \epsilon_i$$

Consequently the external force and moment, which are exerted by the towrope segment $\tilde{\ell}_i$ of the vessel with Bridle, are expressed as follows:

The external force in the y_i direction:

$$T_{1i}' \cos \sigma_{1i} - T_{2i}' \cos \sigma_{2i} \doteq (T_{1i}' - T_{2i}') \frac{B_i}{2\tilde{\ell}_i} = (T_i' \cdot \frac{2\tilde{\ell}_i}{B_i} \epsilon_i) \cdot \frac{B_i}{2\tilde{\ell}_i} = T_i' \epsilon_i$$

Moment around the z_i axis:

$$\begin{aligned} & \frac{T_{1i}' B_i}{2L_i \tilde{\ell}_i} \cdot (f_{1i} + f_{2i}) - \frac{T_{2i}' B_i}{2L_i \tilde{\ell}_i} \cdot (f_{1i} + f_{2i}) \\ &= (T_{1i}' - T_{2i}') \cdot \frac{B_i}{2L_i \tilde{\ell}_i} \cdot (f_{1i} + f_{2i}) \\ &= T_i' \cdot \frac{(f_{1i} + f_{2i})}{L_i} \cdot \epsilon_i \geq \frac{T_i' f_i}{L_i} \epsilon_i \end{aligned} \quad (3)$$

where it is assumed that $(f_{1i} + f_{2i}) \geq f_i$

Next the case when $\epsilon_i > \frac{\pi}{2} - \sigma_{1i}$

will be considered. From the characteristics of the towrope T_{2i}' must be equal to zero and consideration is again given to the equilibrium of forces:

Forces in y_i direction:

$$T_{1i}' \cos\left(\frac{\pi}{2} - \epsilon_i\right) = T_{1i}' \sin \epsilon_i = T_{1i}' \epsilon_i$$

Moment around the z_i axis: (4)

$$\begin{aligned} & T_{1i}' \cdot \frac{f_i}{L_i} \cos\left(\frac{\pi}{2} - \epsilon_i\right) + \frac{T_{1i}' B_i}{2L_i} \cdot \frac{f_{2i}}{\tilde{\ell}_i} \\ &= \frac{T_{1i}' f_i}{L_i} \epsilon_i + \frac{T_{1i}' f_{2i}}{L_i} \epsilon_i \\ &= T_{1i}' \frac{(f_{1i} + f_{2i})}{L_i} \epsilon_i \geq \frac{T_i' f_i}{L_i} \epsilon_i \end{aligned}$$

From comparing (3) and (4) it is clear that both relations are exactly the same. On the other hand from geometric conditions:

$$X_i = X_{i-1} - a_{i-1} - \ell_i - (f_{1i} + f_{2i}) \quad (5)$$

$$Y_i = Y_{i-1} - a_{i-1} \theta_{i-1} - \ell_i \epsilon_i - (f_{1i} + f_{2i} + \ell_i) \theta_i$$

are obtained. Differentiating (5) with respect to time t and assuming that

$$f_i \geq f_{1i} + f_{2i}$$

results in:

$$\begin{aligned} \dot{X}_i &= \dot{X}_0 - \sum_{k=1}^i (\dot{a}_{k-1} + \dot{f}_k + \dot{\ell}_{kk}) = \dot{X}_0 \\ \dot{Y}_i &= \dot{Y}_0 - \sum_{k=1}^i (a_{k-1} \dot{\theta}_{k-1} + f_k \dot{\theta}_k + \dot{\ell}_k \cdot (\dot{\epsilon}_k + \dot{\theta}_k)) \\ &= \dot{Y}_0 - \sum_{k=1}^i (a_{k-1} \dot{\theta}_{k-1} + (f_k + \dot{\ell}_k) \dot{\theta}_k + \dot{\ell}_k \dot{\epsilon}_k) \end{aligned} \quad (6)$$

here X_0, Y_0 are the coordinates of the towing vessel, $T_i', T_{1i}' \dots$ are the values obtained by dividing T_i, T_{1i} by $1/2\rho A_i U_i^2$ where ρ is fluid density, $A_i = d_i L_i$

(L_i vessel length, d_i vessel draft),

U_i vessel forward velocity.

Taking the forward velocity of the towing vessel as U_0 results in:

$$\dot{X}_0 = U_0 \cos(\theta_0 + B_0) = U_0$$

$$\dot{X}_1 = U_1 \cos(\theta_1 + B_1) = U_1 \quad (7)$$

$$\dot{Y}_0 = U_0 \sin(\theta_0 + B_0) = U_0 (\theta_0 + B_0)$$

$$\dot{Y}_i = U_i \sin(\theta_i + B_i) = U_i (\theta_i + B_i)$$

From (6) and (7):

$$\dot{X}_0 = \dot{X}_i = U_0$$

$$\beta_i = \theta_0 + \beta_0 - \theta_i - \frac{1}{U_0} \cdot \sum_{k=1}^i (a_{k-1} \ddot{\theta}_{k-1} + (f_k + l_k) \ddot{\theta}_k + l_k \ddot{\epsilon}_k) \quad (8)$$

Substituting (8) into equations (1) and (2) of [1], after rearranging results in the following equations of motion for the *i*th towed barge:

$$\begin{aligned} & m_{yi} \left(\frac{L_i}{U_i}\right)^2 \cdot \frac{f_i + l_i}{L_i} \ddot{\theta}_i \\ & + \frac{1}{U_i} \left[(m_{yi} - m_i + (k_{i2} + \frac{1}{2}) Y_{\delta i}') L_i + (f_i + l_i) \cdot \right. \\ & \quad \left. \cdot (Y_{\beta i}' + Y_{\delta i}') \right] \ddot{\theta}_i \\ & + \left[Y_{\beta i}' + (k_{i1} + 1) Y_{\delta i}' + T_{i+1}' \right] \theta_i + m_{yi} \frac{L_i}{U_i^2} \cdot \\ & \quad \cdot \sum_{k=1}^i ((a_{k-1} + f_k + l_k) \ddot{\theta}_{k-1}) \\ & + \frac{1}{U_i} \cdot (Y_{\beta i}' + Y_{\delta i}') \cdot \sum_{k=1}^i ((a_{k-1} + f_k + l_k) \ddot{\theta}_{k-1}) \\ & - m_{yi} \frac{L_i}{U_i} \ddot{\theta}_0 - (Y_{\beta i}' + Y_{\delta i}') \theta_0 - T_{i+1}' \epsilon_{i+1} \\ & \quad - m_{yi} \frac{L_i}{U_0} \dot{B}_0 \\ & - (Y_{\beta i}' + Y_{\delta i}') \beta_0 + m_{yi} \frac{L_i l_i}{U_i^2} \ddot{\epsilon}_i + \frac{l_i}{U_i} \cdot \\ & \quad \cdot (Y_{\beta i}' + Y_{\delta i}') \dot{\epsilon}_i \\ & + T_i' \epsilon_i - T_{i+1}' \epsilon_{i+1} + m_{yi} \frac{L_i}{U_i^2} \cdot \sum_{k=1}^i (l_{k-1} \ddot{\epsilon}_{k-1}) \\ & + \frac{1}{U_0} (Y_{\beta i}' + Y_{\delta i}') \cdot \sum_{k=1}^i (l_{k-1} \dot{\epsilon}_{k-1}) = 0 \end{aligned}$$

$$\begin{aligned} & n_i \left(\frac{L_i}{U_i}\right)^2 \ddot{\theta}_i \\ & + \frac{1}{U_0} \cdot \left[(N_{ri}' + (k_{i2} + \frac{1}{2}) N_{\delta i}') L_i - (f_i + l_i) \cdot N_{\beta i}' \right. \\ & \quad \left. - N_{\delta i}' \right] \ddot{\theta}_i \\ & + \left[(k_{i1} + 1) N_{\delta i}' - N_{\beta i}' \right] + \frac{a_i}{L_i} \cdot T_i' \theta_i \\ & - \frac{1}{U_i} (N_{\beta i}' - N_{\delta i}') \cdot \sum_{k=1}^i [(a_{k-1} + f_{k-1} + l_{k-1}) \ddot{\theta}_{k-1}] \\ & - T_i' \frac{f_i}{L_i} \epsilon_i - T_{i+1}' \frac{a_i}{L_i} \epsilon_{i+1} - \frac{1}{U_i} (N_{\beta i}' + N_{\delta i}') \dot{\epsilon}_i \\ & - T_{i+1}' \frac{a_i}{L_i} \theta_{i+1} + (N_{\beta i}' - N_{\delta i}') \theta_0 + (N_{\beta i}' - N_{\delta i}') \beta_0 \\ & - \frac{1}{U_i} (N_{\beta i}' - N_{\delta i}') \cdot \sum_{k=1}^i (l_{k-1} \dot{\epsilon}_{k-1}) = 0 \end{aligned} \quad (10)$$

These relations are exactly the same as equations (5) and (6) of [1] when f_i is taken as the length to the tip of the bridle and l_i is taken as the length of towrope from the tip of the bridle.

IV INVESTIGATION OF COURSE STABILITY PERFORMANCE OF TOWED VESSELS BY TOWING VESSELS BY TOWING EXPERIMENTS

The quality of the towed vessel course stability performance changes with the size of the towing vessel and towed vessel as shown in Fig.2. However, it does not follow that the course stability of the towing ship-towed vessel system is equal to the towed vessel course stability performance when towed by the towing tank carriage. Therefore, a towing ship - towed vessel system should be used when investigating the course stability performance. (Here the towing ship-towed vessel system designates the towing vessel and all towed vessels.)

To investigate the course stability of the system a study was conducted by changing the towrope length and examining the path of the vessels.

Naturally, it is preferable to calculate the course stability performance using the towed vessel(s) and towing vessel's derivatives. However since the course stability performance is qualitatively shown in Figs.2, 3, and 4, experiments were conducted to determine the minimum tow rope length namely the limit of the course stability of the system. The models used are described

in Table 1. The skegs were fitted in pairs. Two types of skegs were used: the Mariner skeg with a symmetric air-foil section and the Deformed skeg with a chambered air-foil section which are shown in Fig. 5.

Table 5

	Tugboat	Barge
L_{pp}	0.800m	2.500m
B	0.228m	0.600m
d	0.027m	0.143m
Displ.	0.436kg	188.26kg
C_B	0.651	0.875

$$U = 0.367\text{m/s}, F_n = 0.07423$$

In the experiments radio controlled steering was used. The towrope length was changed and the model ship's course stability performance was investigated by photographing the towing path while the model moved forward. These results are shown in Figs. 7, 8, and 9 while a comparison for $q=l/L=2$ is presented in Fig. 10. The results are:

- 1) Without the skegs the course stability performance is poor, so that whatever l is used, straight line towing is not possible.
- 2) With the Mariner skeg when $l > 6L$, straight line towing is possible, while with a shorter towrope length it is impossible.
- 3) With the Deformed skeg there is adequate stability for straight line towing when $l > L_1$.

Consequently although the deformed skeg has a slightly higher value of resistance than the mariner skeg in forward motion, it enables course stable performance to be achieved with a short towrope.

V EXPERIMENTAL STUDY FOR IMPROVING THE COURSE STABILITY PERFORMANCE OF A SINGLE TOWED VESSEL.

One way to improve the course stability performance of the towing ship-towed vessel system is to improve the course stability performance of the individual vessels. Consequently the various improvements from the mariner, deformed, slotted flap and slotted flap with rotor skegs were investigated, Figs. 5, 6, and 7, to determine the best skeg type.

(1) Investigation Using Free Running Models

It is known that when a model which was towed from a towing tank carriage at constant speed is used in free running

tests there is a reduction in the model's speed, and it has a slightly poorer course stability performance. To simply decide the relative characteristics of skegs free running model tests were used.

Figs. 11 to 14 present the paths of the free running models when the skegs are fitted to the barge. From Fig. 10, it is clear that without skegs, a straight line path does not occur and the stability performance is bad. It is also evident that the course stability performance improves when the mariner skegs or deformed skegs are fitted. The course stability performance with the deformed skegs is better than when the mariner skegs are fitted.

Fig. 11 shows the results from using the slotted flap skeg. From this figure when η increases the stability performance is improved. Thus when $\eta > 20^\circ$ a straight running is possible. However, when $\eta > 70^\circ$ stalling occurs, and the stability performance becomes poor. The model paths of the case when the slotted flap skegs with rotors are fitted are shown in Fig. 12. The turning rotor causes a high lift force. In addition, when η is increased, the stability becomes better so that even when $\eta > 70^\circ$ good results are obtained. A comparison of slotted flaps skegs with and without rotor action is shown in Fig. 18. When η is small the turning rotor does not cause a large difference, but when $\eta > 70^\circ$ its effect is clear. Therefore, it is understood that the turning rotor causes a large lift force and the course stability performance improves. From these experiments, it is therefore anticipated the stability performance is improved by skegs in the following order:

Mariner skeg Slotted flap skeg
Deformed skeg Slotted flap skeg with
rotors [best]

(2) Oblique Towing Experiments

To determine the hydrodynamic forces in each case, the improvement in the course stability performance of the barge model was investigated by comparing the effects of the various kinds of skegs on the hull.

This was done by oblique towing experiments. These tests were made using the carriage of the University of Kyushu's Faculty of Engineering Naval Architecture's ship motion basin. The skegs used in these tests are shown in Figs. 5 and 6. For the case of the slotted flap skegs with rotors experiments were made by changing the revolutions ω of the rotor as shown in Table 2.

ω	η						
	0°	5°	10°	20°	30°	50°	70°
0	o	o	o	o	o	o	o
800	o	o	o	o	o	o	o
2000	o	o	o	o	o	o	o

Table 2

The skegs shown in Fig.5 were fitted to both sides of the bottom of the barge stern. They form the three-component force measurements at midships, the hydrodynamic forces in the x and y axis and the moment around the z axis were measured to obtain Y'_β and N'_β

	Without skeg	Mariner skeg	Deformed skeg
X'	0.04316	0.04711	0.05409
Y'_β	0.3124	0.3210	0.3672
N'_β	0.1428	0.0937	0.0607

Table 3

The experimental results are shown in Figs.15 to 25 and the corresponding Y'_β and N'_β values are shown respectively in Figs. 24 and 25. Table 3 summarizes the values of X' , Y'_β and N'_β with no skegs, mariner skegs and deformed skegs. When the mariner skeg and deformed skeg are fitted to the barge, there is not a very large difference in the values of Y'_β in comparison with the large differences in the values of N'_β . When the deformed skegs are used, it clear there is a remarkable reduction in the N'_β value and a large contribution to Δ . In addition, when the slotted flap skeg is fitted there is a remarkable increase in the values of Y'_β with increasing η . It is clear the value of N'_β is negative when η is near 0°, as shown in Fig.25, and stall occurs when $\eta > 10^\circ$. As Fig.5 indicates as the rotation energy is supplied preventing stall so a high lift force results. Although there is an increase in Y'_β when both ω and η become larger in Fig.24, there is little noticeable difference in the value of N'_β in Fig.25. Finally it is anticipated that the course stability performance is increased by skegs in the following order:

Mariner Skeg, Slotted flap skeg
Deformed skeg Slotted flap skeg with rotor

only a small effect.

IV CONCLUSION

From the previous results the following conclusions were obtained.

1) The major effects of the skegs on the course stability performance are to increase L'_β and to decrease N'_β , as well as causing a slight increase in resistance. Consequently, it is conceivable that the stability performance becomes good when a high lift skeg such as the slotted flap skeg is used.

2) In straight line towing in the towing tank where the towed vessels are towed from the carriage, the effective towing vessel becomes extremely big and the towed vessel extremely small. As Figs. 2 and 3 indicate this represents a situation different from the actual one. Therefore to investigate the course stability performance of the towing ship-towed vessel system, it is necessary to conduct the experiments using a towed vessel system in an installation with a large unrestricted water surface.

The authors express their sincere thanks to Messrs. Nagiri, Yamada, and Yamamoto for their cooperation in experiments.

REFERENCES

- 1) Inoue, S. and et.al., "The Course Stability of Towed Boats," Journal of the Society of Naval Architects of West-Japan, No. 42, July, 1971 pp.11-25 [In Japanese]
- 2) Inoue, S. and Lim, S., "The Course Stability of Towed Boats(continued)," Journal of the Society of Naval Architects of West Japan, No.43, March 1972, pp. 35-44 [In Japanese]
- 3) Inoue, S. and Lim S., "The Course Stability of Towed Boats-When the Mass of the Towing Ship is Considered," Journal of the Society of Naval Architects of West Japan No.44. August 1972, pp. 29-34 [In Japanese]
- 4) Inoue, S. and Lim S., "The Course Stability of Towed Boats-Effect of the Towing Points and Restricted Water," Journal of the Society of Naval Architects of West Japan, No.46, August 1973 pp.25-31. [In Japanese]
- 5) Winnifred R. Jacobs, "Estimation of Stability Derivatives and Indices of Various Ship Forms and Comparison with Experimental Results," Davidson Laboratory, D.D.C. September 1964 pp.7-11.

6) Lim, S., "On the Steady Turning of Towed Ship System," Journal of the Society of Naval Architects of Japan Vol.137, June 1975, pp177-185. [In Japanese] English Version published in Selected papers from the Journal of Society of Naval Architects of Japan Vol. 14, 1976 pp. 43-55.

7) Inoue, S. and et.al. "Some Considerations on Tanker Model-Ship's Emergent Steering Avoidance," Journal of the Society of Naval Architects of West-Japan, No.44, August 1972, pp.83-94. [In Japanese]

TRANSLATOR'S NOTE: The Interested reader can obtain a summary of [1],[2],[3],[4] in:

Inoue, S., and Lim, S., "The Manoeuvrability of Towed Ships System," PROCEEDINGS 14th International Towing Tank Conference, Vol. 2, Ottawa, Canada, 1975. pp. 571-580.

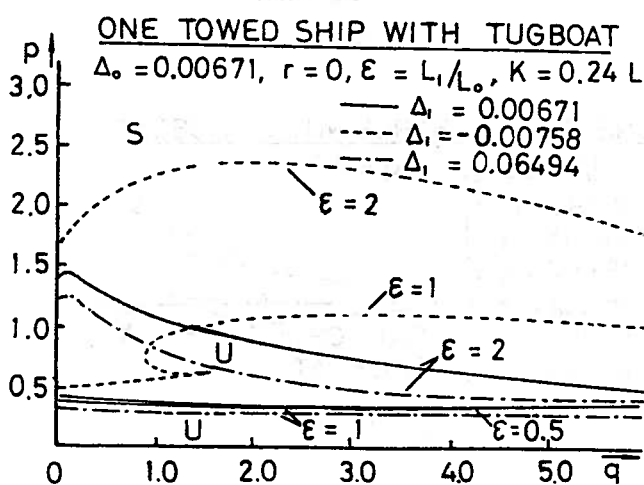
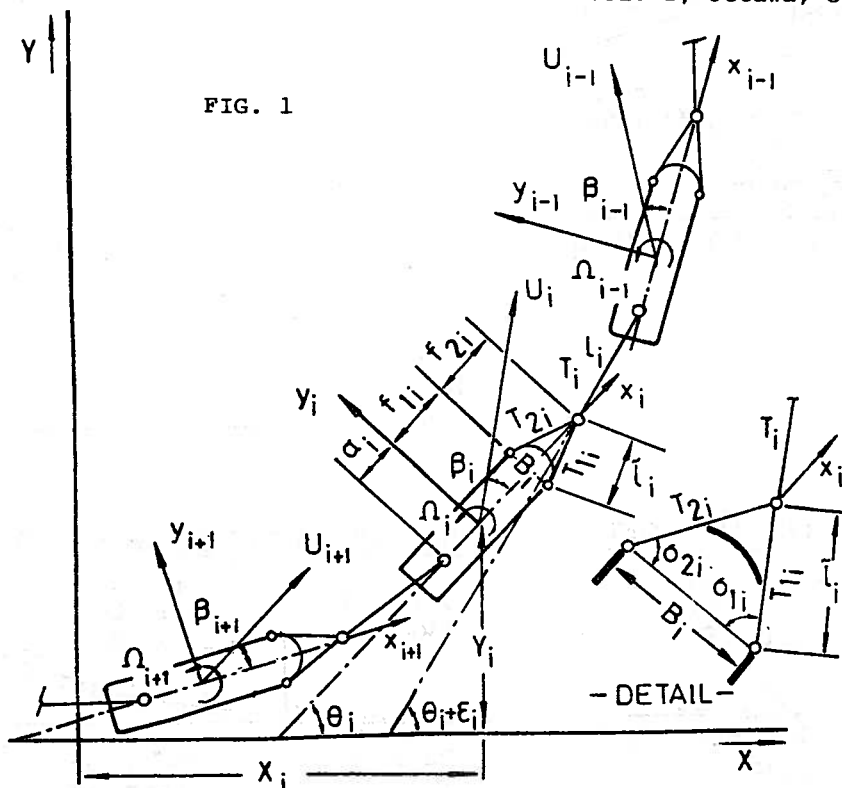


FIG. 2

Notation: $q = l/L$
 $p = f/L$

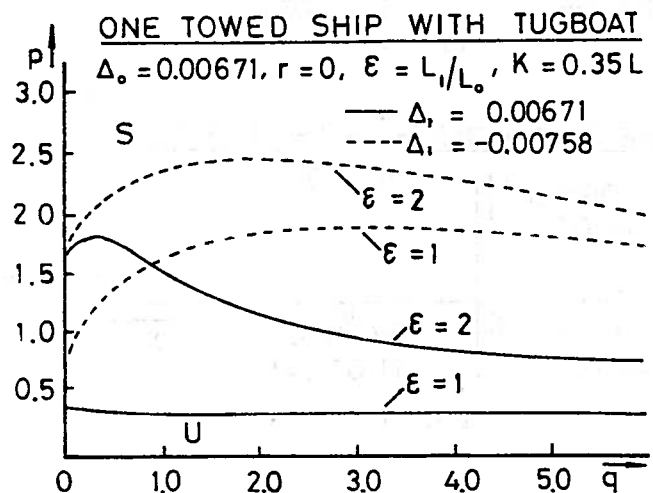


FIG. 3

L : Towed Vessel Length.
 l : Length of towing rope between vessels.
 f : Distance from center of gravity to fore towing pt.

ONE TOWED SHIP WITH TUGBOAT

$\Delta_0 = 0.00671, r = 0, K = \text{Radius of Gyration}$

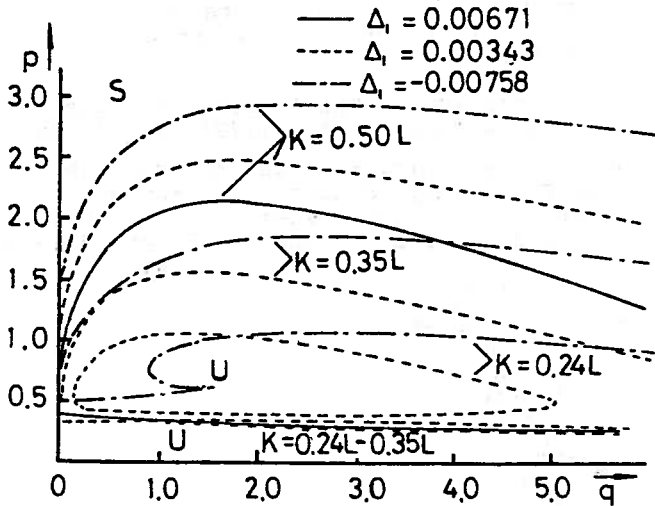


FIG. 4

(Notation as in Figs. 2 and 3)

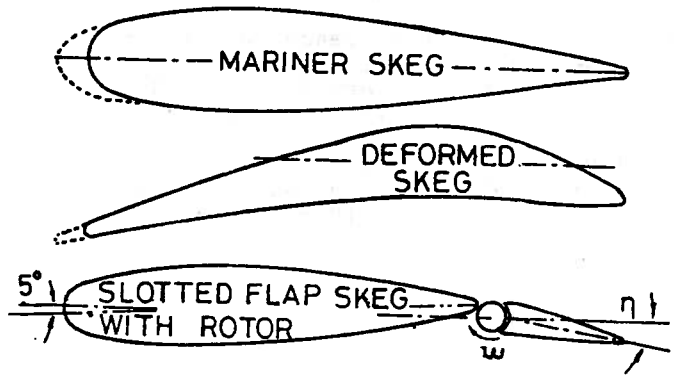
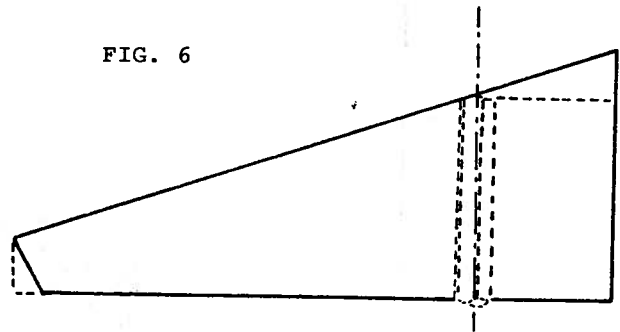


FIG. 5

FIG. 6



ONE TOWED BARGE WITH TUGBOAT

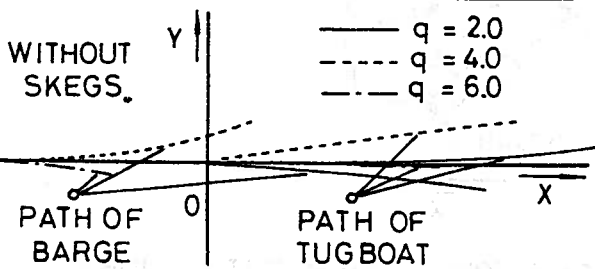


FIG. 7

ONE TOWED BARGE WITH TUGBOAT

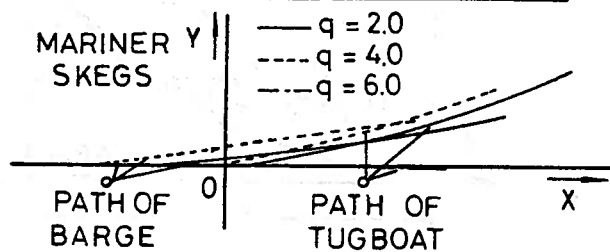


FIG. 8

ONE TOWED BARGE WITH TUGBOAT

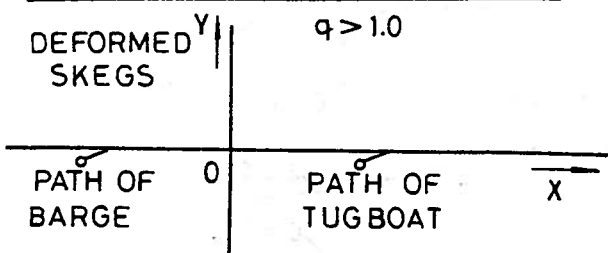


FIG. 9

ONE TOWED BARGE WITH TUGBOAT

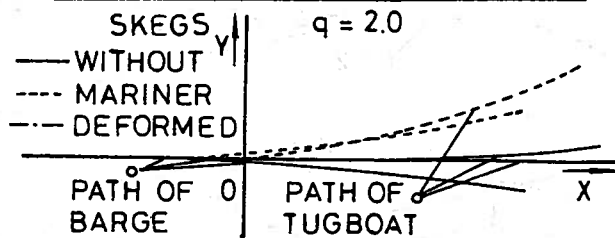


FIG. 10

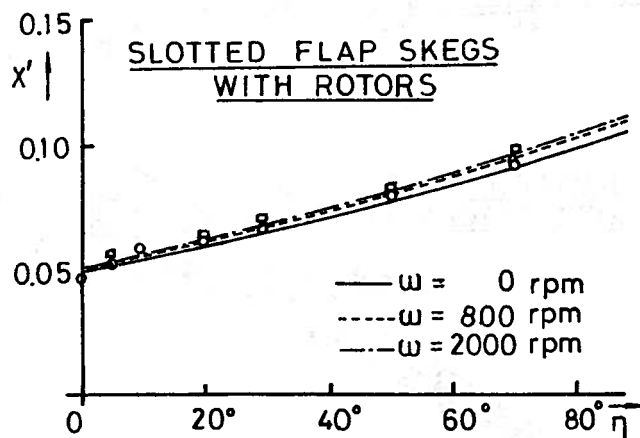
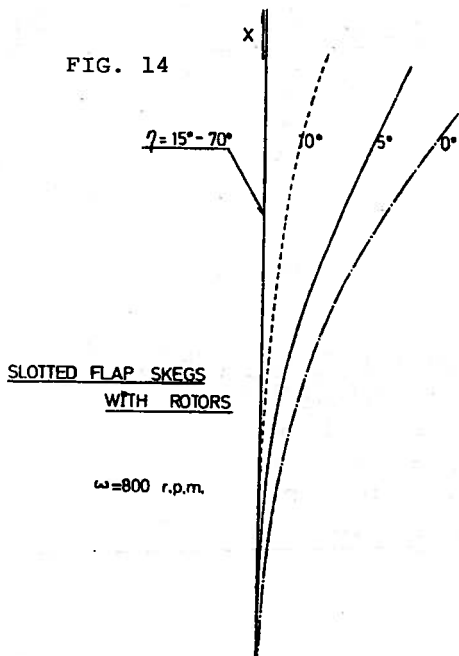
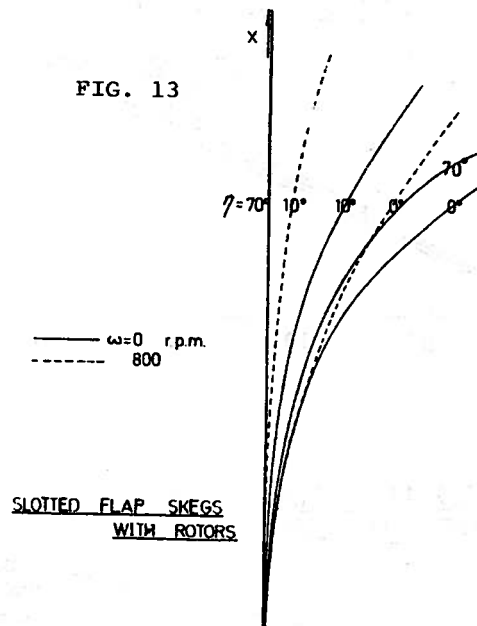
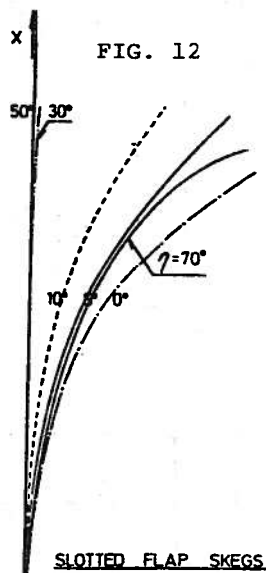
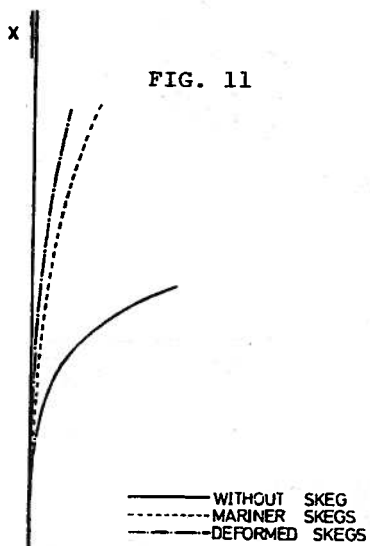


FIG 15

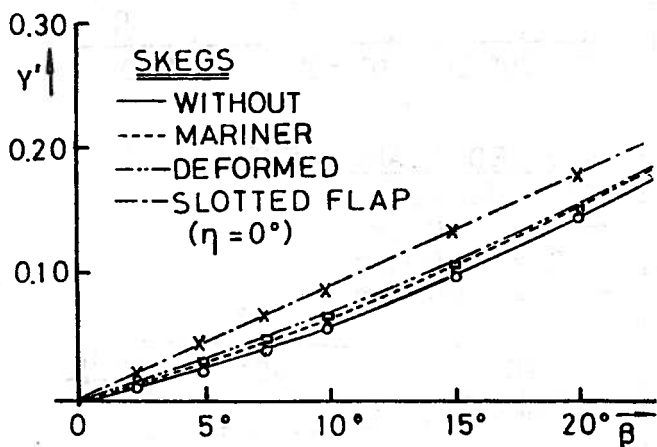


FIG. 16

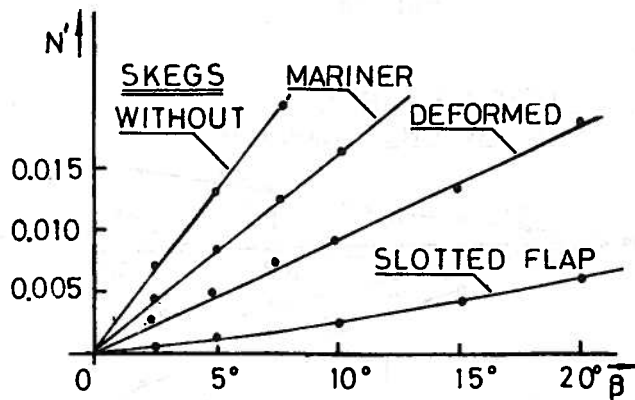


FIG. 17

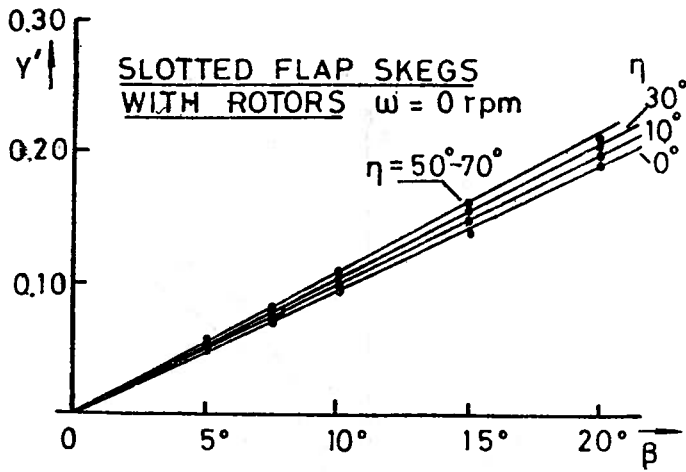


FIG. 18

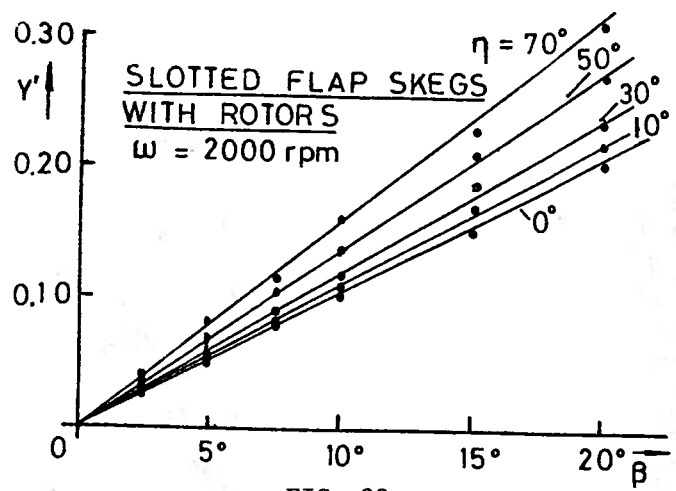


FIG. 22

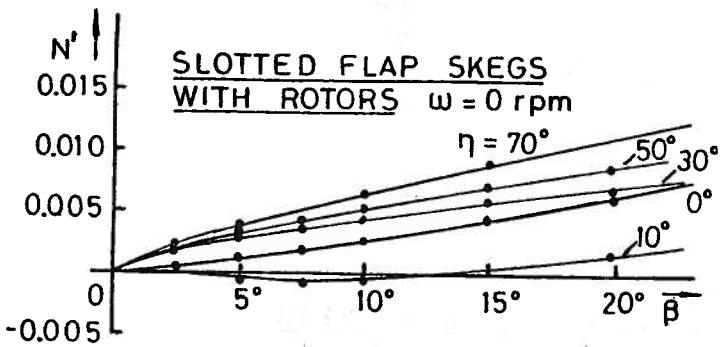


FIG. 19

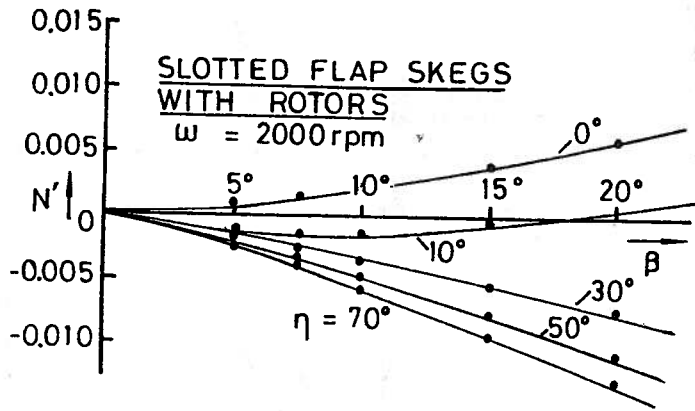


FIG. 23

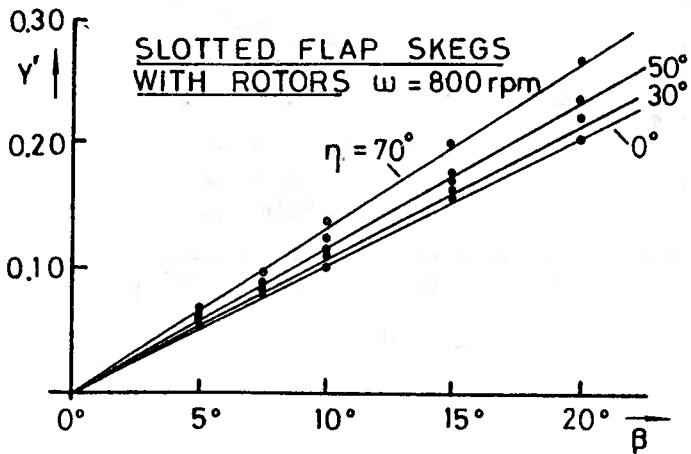


FIG. 20

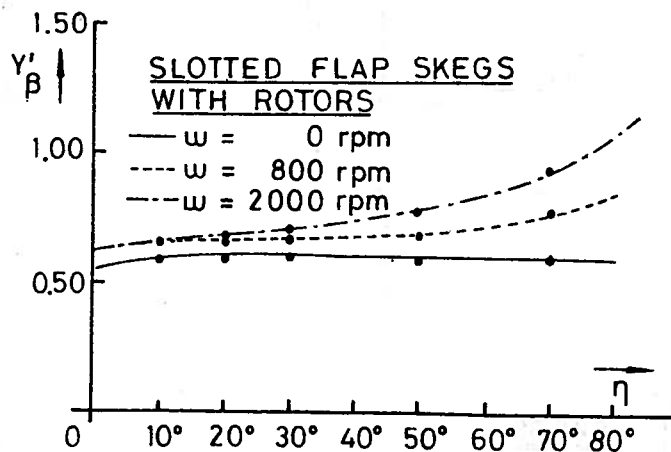


FIG. 24

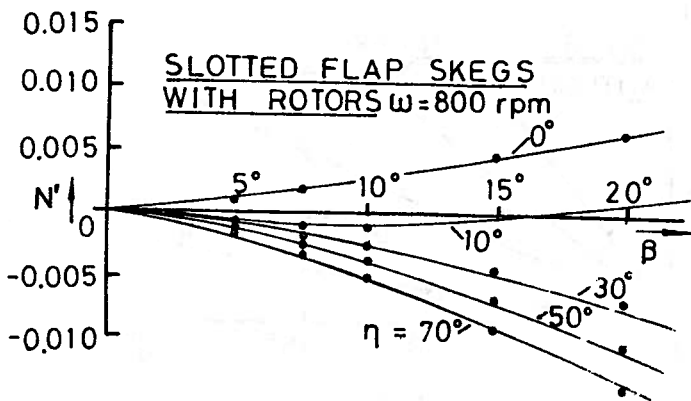


FIG. 21

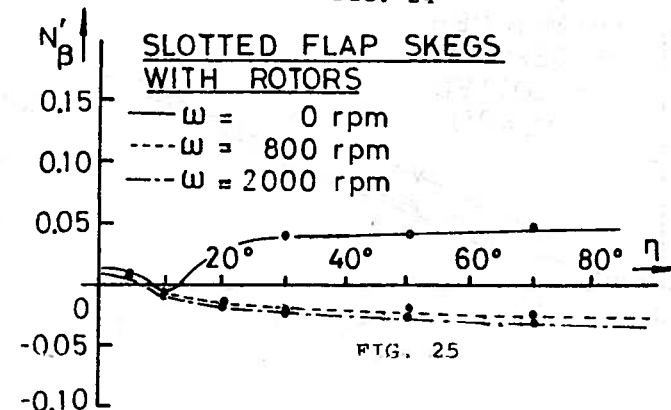


FIG. 25

ON THE COURSE STABILITY OF A BARGE¹

BY

S. INOUE²
K. KIJIMA²
M. DOI²

ABSTRACT

A barge has been used for elimination or reduction of labor in loading and unloading work, or for specialized purposes. Recently, their size is growing more and more, and they have a great variety. Because a barge generally is course unstable, various ways for stabilization have been considered. One of the well known ways is the skeg fitted on aft of the barge.

In this paper, the skeg effect on the course stability on a barge is investigated experimentally by measuring the lateral force and moment acting on hull and skeg. The types of skeg selected are the following:

- (1) Mariner Type Skeg, (2) Deformed Type Skeg
- (3) Slotted Flap Type Skeg.

From these results, we may conclude that the lateral force acting on a barge increases with greater distances between skegs but the moment decreases, and the difference due to skeg type is very remarkable. We see that a barge with skeg becomes more stable in order of Marine Type Skeg, Deformed Type Skeg and Slotted Flap Type Skeg. However, there is a remarkable difference in static derivatives in oblique towing tests, especially in the value of N'_8 .

It is not necessary to consider the interference effect between skeg and ship's body on the hydrodynamic derivatives in the case of large separation distance between skegs.

The most desirable method for the course stabilization of the barge will be to select the Slotted Flap Type Skeg. However, it should be noted that there is a remarkable increase in the resistance of barge due to skegs. Therefore, when applying these results to the actual vessel we should have to consider the most suitable method for the course stabilization of a barge in connection with the lateral force and moment and the resistance increment of the barge to skegs.

TRANSLATION³

1. INTRODUCTION

From ancient times barge vessels have been considered as an economical and rational means of ocean borne transportation. Recently, in addition to transport, special barges are being built. The barge vessels used in transport work are of two major types; one is the towed barge and the other is the pushed barge. The towed barge hulls are basically simple hull forms and their course stability performance is poor. The barges are course unstable due to the hull form design which causes safety and navigation problems when towing.

The recently constructed large barge vessels typically have a spoon bow, a stern with the dead wood cut away, and they are basically very course unstable. Among the various methods considered for improving the course stability performance, the main one is to install skegs to the dead wood cutaway section of the stern.

While many types of skeg designs and types have been used on full scale vessels, there have been hardly any formal publications in research journals regarding the performance of the skegs.

The authors [1] previously conducted an investigation of the course stability performance of a barge vessel in a towed vessel system. In this present paper a discussion of the results of an experimental investigation of the influence of the skegs, their form and location on the course stability performance, and interaction of the hull and skegs is presented for a towed barge system.

¹TRANSACTIONS OF THE WEST-JAPAN SOCIETY OF NAVAL ARCHITECTS, No. 54, August 1977, pp. 193-201

²Faculty of Engineering, Kyushu University

³Prepared by Robert Latorre, Dept. of Naval Naval Architecture and Marine Engineering University of Michigan, Ann Arbor, Michigan

2. FORM OF MODEL HULL AND SKEGS

The model used in the experiments is a barge hull whose main particulars and hull form are shown in Table 1 and Fig. 1. The three types of skegs used in this report are shown in Table 2 and Fig. 2. Each of these three skegs has a vertical projected area which is nearly the same profile as the deadwood cutaway from the barge. From their horizontal cross-section the skegs can be distinguished as: the Mariner type skeg (M.T.S.) with a symmetrical airfoil section, the Deformed type skeg (D.T.S.) with a cambered airfoil section and the slotted flap type skeg (S.F.T.S.). The slotted flap type skeg has the same amount of camber as the D.T.S. and has two slots at the two flap locations. The skegs are set in pairs symmetrically around the vessel's centerline near the vessel's sides.

L_{pp} :	2.5m
B :	0.60m
d :	0.1417m
C_b :	0.875
Δ :	185.98kg

Table 1 Particulars of Barge Model

Length :	0.25m
Area :	0.01635m ²
Area Ratio :	1/22
Aspect Ratio :	0.524

Table 2 Particulars of Skegs

3. EXPERIMENTAL METHOD AND MEASUREMENT RESULTS

In determining the course stability performance of a barge with skegs, it is necessary to know the hydrodynamic forces acting on the vessel and its hull motion. Therefore, the hydrodynamic forces were measured in oblique towing tests and rotating arm turning tests of captive models.

In order to investigate the influence of the skeg forms and spacing, the hydrodynamic forces were measured for the following four cases in the experiments:

1. Hydrodynamic forces acting on the barge hull without skegs.
2. Hydrodynamic forces acting on the barge hull with skegs.
3. Hydrodynamic forces acting on the skeg fitted to the barge aft (stern).
4. Hydrodynamic forces acting on the skeg alone.

The model velocity was $U=0.3$ m/s which is scaled from the actual barge being towed at 5 knots. In the tests the coordinate system in Fig. 3 was adopted in order to measure the hydrodynamic forces as well as the skeg location.

The spacing between the skeg locations b_s is expressed in a non-dimensional parameter $\eta = b_s/B$ using the vessels beam (B). In the tests four values of η were used: 0.33, 0.50, 0.67, 0.75. The maximum value of η was 0.75 which was determined from the hull form and the arrangement of the skegs on the model.

3.1 The Hydrodynamic Forces Acting on the Barge Hull With and Without the Skegs

The measurement results of the hull side force (Y) and the moment around midships (N) for the drift angle β are shown in non-dimensional form in Figs. 4-10, where:

$$Y' = Y/1/2\rho L d U^2$$

$$N' = N/1/2\rho L^2 d U^2$$

It is clear that there is a remarkably large difference in the side force and moment for the vessel with and without the skegs. The hydrodynamic derivatives obtained from this data are shown in Figs. 11 and 12 and the center of pressure for these cases is shown in Fig. 13.

3.2 Hydrodynamic Forces Acting on the Skeg Behind the Hull.

The hydrodynamic forces acting on the skeg fitted behind the barge vessel were measured in the same manner as previously described. From these results the hydrodynamic derivatives of the side force and moment denoted by ${}_s Y'_\beta$ and ${}_s N'_\beta$ were obtained and shown in Figs. 14 and 15.

As for the value of ${}_s Y'_\beta$, when the skeg spacing η changes there is a noticeable change with all three types of skegs.

3.3 Hydrodynamic Forces acting on the Skeg in Open Water

The static derivative of the side force and moment of a pair skeg denoted by ${}_o Y'_\beta$ and ${}_o N'_\beta$ are shown in Figs. 16 and 17.

As for the value of ${}_o Y'_\beta$ there are only small differences between the three types of skegs, M.T.S., D.T.S., and S.F.T.S. when the spacing of the skegs is small. However, when η becomes large the S.F.T.S., exhibits a large value. While there are small effects on ${}_o N'_\beta$ from varying η , there are remarkable differences between the S.F.T.S. values and those of the other skegs.

4. INFLUENCE OF SKEG SPACING

The previously described relationship of the side force and moment derivatives of the hull and skeg spacing are summarized in Table 3. From these results the value of Y'_β becomes larger in the following order: M.T.S., D.T.S. and S.F.T.S. while the value of N'_β becomes correspondingly smaller in that order. In addition the corresponding center of pressure moves back. This is especially evident in the case of S.F.T.S. where the center of pressure moves back from midships as the skeg spacing becomes wider. This represents improved stability from the viewpoint of the vessel's course stability performance. Consequently it is good to use skegs whose spacing is as wide as possible.

5. MUTUAL INTERACTION OF SKEG AND HULL

First, in order to study the effect of the hull on the skeg, comparisons are made between the ratio of the hydrodynamic derivatives s'_β and s'_β for the skegs behind the hull and the hydrodynamic derivatives o'_β and o'_β for the skegs in open water. These are shown in Figs. 18 and 19.

The influences of the hull on the MTS and DTS are evident irrespective of the value of η , and the ratio of the side force derivatives becomes

$$s'_\beta / o'_\beta \approx 1/2$$

while the hull effects on the SFTS skeg are not apparent except at large values of η . As for the moment around the skeg axis, the influence of the hull on each of the three types of skegs is present and it depends mainly on the value of η . It seems that this tendency is mainly caused by differences in flow around the stern

Type of Skeg		η				Without Skeg
		0.75	0.67	0.50	0.33	
Y'_β	Mariner	0.34	0.30	0.30	0.30	0.26
	Deformed	0.47	0.37	0.34	0.33	
	Slotted Flap	0.62	0.62	0.47	0.43	
N'_β	Mariner	0.098	0.103	0.114	0.128	0.153
	Deformed	0.065	0.070	0.104	0.104	
	Slotted Flap	-0.040	-0.028	0.031	0.047	
N'_β / Y'_β	Mariner	0.288	0.343	0.308	0.427	0.588
	Deformed	0.138	0.189	0.306	0.315	
	Slotted Flap	-0.065	-0.045	0.066	0.109	

Table 3 - Derivatives

which are related to the deadwood cutaway from the stern.

Table 4 - Skeg Effect ($B_s Y'_\beta / B Y'_\beta$ in %)

Type of Skeg	η : 0.75	0.67	0.50	0.33
Mariner	12.1	18.2	19.7	19.7
Deformed	16.4	22.8	18.0	16.5
Slotted Flap	30.0	33.6	39.8	35.3

Type of Skeg	η : 0.75	0.67	0.50	0.33
Mariner	0.95	1.04	0.89	1.48
Deformed	1.34	1.19	0.89	1.27
Slotted Flap	0.83	0.56	0.56	0.83

Table 5: Skeg Effect ($B_s N'_\beta / B N'_\beta$ in %)

Then in order to study the amount the skeg contributes to the barge hull, the hydrodynamic derivatives of the hull without the skegs $B Y'_\beta$ and $B N'_\beta$ and the hydrodynamic derivatives of the hull with the skegs $B_s Y'_\beta$ and $B_s N'_\beta$ were obtained, and the values of $B_s Y'_\beta / B Y'_\beta$ and $B_s N'_\beta / B N'_\beta$ are given in Tables 4 and 5. Here the S.F.T.S. has the largest contribution of 30% at $\eta = 0.7$. In addition, irrespective of the skeg type the effects are large when the values of η are small. It can be said that when η is small there is an effective interaction of the skegs with the stern flow pattern. While for the moment, irrespective of the skeg type, M.T.S. and D.T.S. or S.F.T.S. and value of η the contributions are small. Thus, it is possible to express the hydrodynamic derivatives of the hull motion with skegs by introducing the interaction coefficients of the hull and skegs as follows:

$$Y'_\beta = B Y'_\beta + C_1 \frac{A_s}{L_d} o'_\beta \quad (1)$$

$$N'_\beta = B'_N N'_\beta - C_2 \frac{A_s}{Ld} \left[\frac{\ell}{L} \circ Y'_\beta + \frac{L_s}{L} \circ N'_\beta \right] \quad (2)$$

where

- B'_Y : Y'_β for the hull without the skeg
 $\circ Y'_\beta, \circ N'_\beta$: Hydrodynamic Coefficients of Skeg in Open Water
 ℓ : Distance from midships to the axis of the skeg moment
 L_s : Skeg Length
 A_s : Skeg Profile Area
 C_1, C_2 : Interaction Coefficients

The interaction coefficients C_1 and C_2 are presented in Table 6. When the spacing between skegs becomes large, the values of C_1 and C_2 become nearly equal to 1.0 and the interaction with the hull can be ignored.

Table 6 - Values of C_1 and C_2

Type of Skeg	η :	0.75	0.67	0.50	0.33
C_1	Mariner	1.07	0.46	0.42	0.42
	Deformed	1.05	0.70	0.73	0.73
	Slotted Flap	0.97	0.87	0.58	0.58
C_2	Mariner	1.14	0.79	0.53	0.56
	Deformed	1.04	0.90	0.67	0.75
	Slotted Flap	1.03	0.82	0.64	0.67

6. SKEGS AND COURSE STABILITY PERFORMANCE

In the previous section the oblique towing test results were used to determine the towed vessel stability performance to a certain degree. In this section the effect of the skeg on the course stability is studied using the general expression for Δ to decide the course stability performance:

$$\Delta = Y'_\beta \cdot N'_r - (m_x - Y'_r) \cdot N'_\beta \quad (3)$$

Type of Skeg	Y'_β	N'_β	$m_x - Y'_r$	N'_r	Δ
Without	0.26	0.146	0.449	0.014	-0.06919
Mariner	0.34	0.098	0.275	0.039	-0.0137
Deformed	0.47	0.065	0.235	0.052	0.0092
Slapped Flap	0.62	-0.040	0.285	0.044	0.0205

Table 7 - Course Stability ($\eta = 0.75$)

From the results of the investigations in the previous section, the skegs were most effective when $\eta = 0.75$ and for this condition rotating arm turning tests were made to obtain the values of Y'_r and N'_r . These

results are shown in Table 7 and the following comparison of the course stability was obtained from this table.

When the M.T.S. is fitted to a hull whose course stability performance was originally unstable, the performance is slightly improved and the hull may be called slightly unstable. When the D.T.S. is fitted to this hull, the stability is further improved and the hull may be called slightly stable. The SFTS causes the hull to become extremely stable. Comparing the effect on the hull from D.T.S. and SFTS, it appears there is not a large variation in the turning derivatives, but there is a large difference in the static derivatives for oblique motion tests. This is especially obvious in the variation in N'_β . Consequently, from considering only the course stability performance, it appears that the SFTS gives the maximum effect.

However, there is another problem that when the skegs are fitted the resistance increases. Assuming that the barge is usually towed at about 5 knots, the corresponding added resistance of the barge with each type of skeg are shown in Table 8. Examining this comparison of the barge hull resistance with-without skegs, when the SFTS are fitted there is an increase of 40% in the resistance. However, with the D.T.S. this increase is limited to 10%. In practice there are many cases in which it is necessary to fit skegs to the barge and since there is hardly any noticeable difference between the D.T.S. and the M.T.S. with symmetric airfoil section, it appears that since the D.T.S. contributes more stability from considerations of course stability the D.T.S. is the best skeg from resistance and course stability considerations.

Consequently, it is necessary to include consideration of not only the side force and moment caused by the skeg fitted to the towed barge but also the skegs' resistance. Consequently, when developing the optimum skeg design for actual vessels both of these aspects should be used in the evaluation.

Without Skeg	1.0	-
Mariner Type Skeg (MTS)	1.07	1.0
Deformed Type Skeg (DTS)	1.11	1.01
Slotted Flap Type Skeg (SFTS)	1.40	1.30

$\eta = 0.75$, $U = 5$ knots

Table 8 Rate of Resistance Increase

7. CONCLUSIONS

In the above investigation, the method of using skegs to improve the course stability performance of an unstable barge hull form was studied. The skegs caused different degrees of improvement in the course stability performance depending on the type of skeg and the position of its installation. For the three types of skegs examined, the course stability performance became increasingly better by using: Mariner Type Skegs (MTS), Deformed Type Skegs (DFS), and Slotted Flap Type Skegs (SFTS). It was also shown that the course stability performance would improve as the skeg spacing increased.

The SFTS caused the largest course stability improvement among the skegs examined. However, using this skeg type results in a large increase in the towing resistance. Consequently it can be

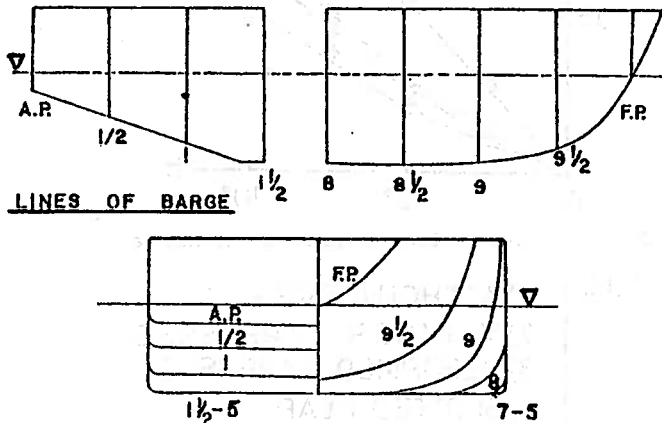


FIG. 1 Plan of Model Barge

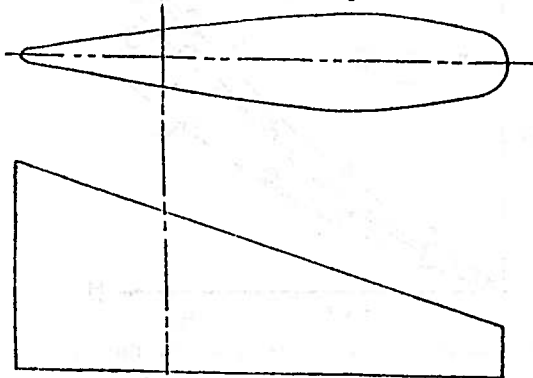


FIG. 2-1 Mariner Type Skeg

concluded that it is worthwhile to use the SFTS to improve the barge course stability when it is possible to accept the added resistance from these skegs. However, it is better to use the DFS in order to reduce the added resistance if it is possible to accept a smaller course stability.

Finally, giving consideration to the skeg performance (resistance and course stability improvement) is useful when studying the towed barge.

The authors would like to express their sincere thanks to Messrs. Murakami, Katsuno, and Nagiiri for their cooperation in making the experiments as well as to Mr. Todo who conducted these experiments as part of his graduation thesis.

LITERATURE

1. Inoue, S., et. al., "Some Studies of the Course Stability of Towed Ships Systems," TRANSACTIONS OF THE WEST JAPAN SOCIETY OF NAVAL ARCHITECTS, No. 50, August, 1975. pp. 65-74. [In Japanese]
TRANSLATION: Improving Barge Towing Translation No. B-I-2, R. Latorre

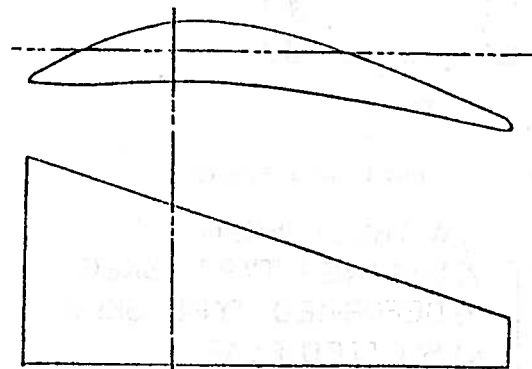


FIG. 2-2 Deformed Type Skeg

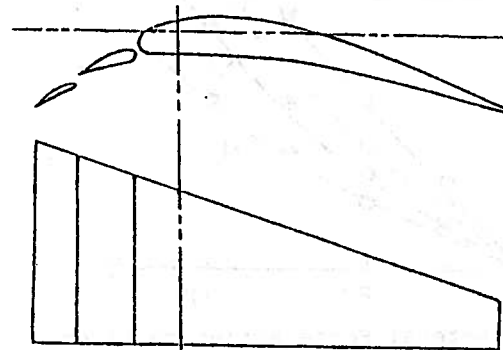


FIG. 2-3 Slotted Flap Type Skeg

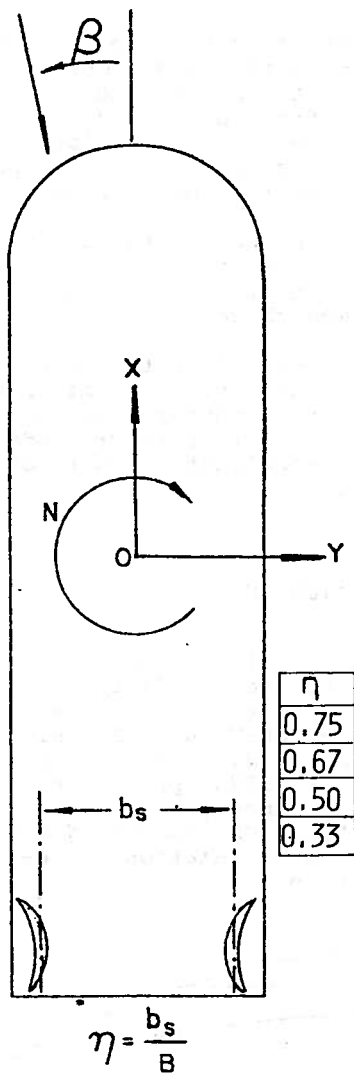


FIG. 3 Coordinate System

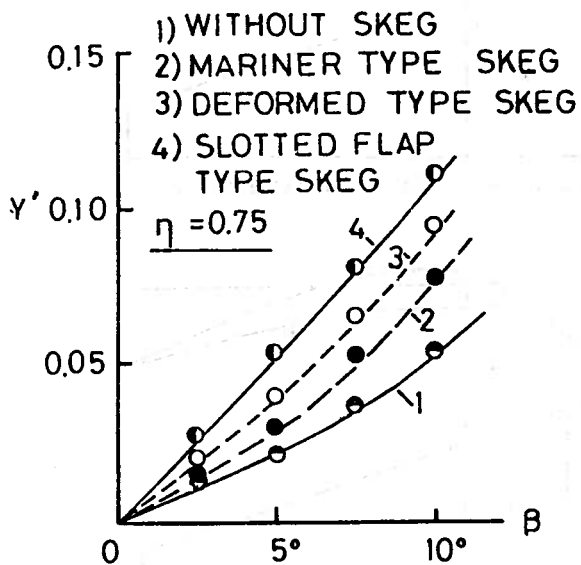


FIG. 4 Lateral Force Acting on Barge

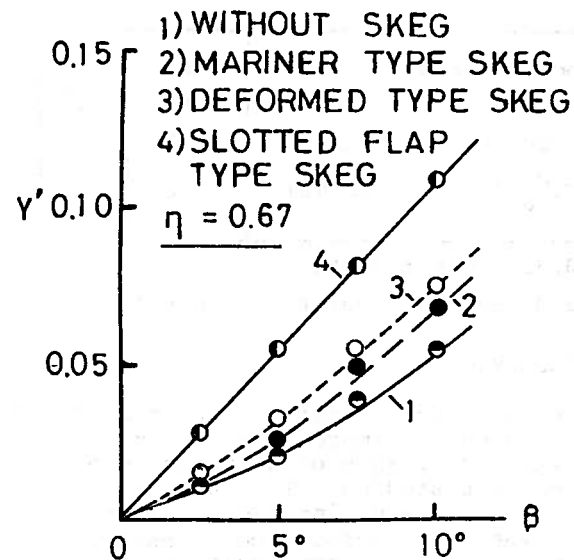


FIG. 5 Lateral Force Acting on Barge

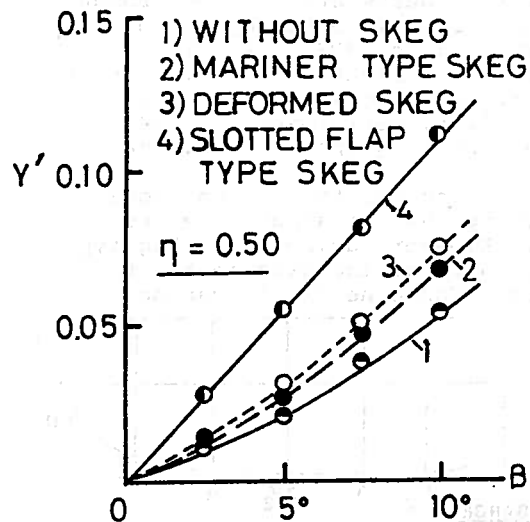


FIG. 6 Lateral Force Acting on Barge

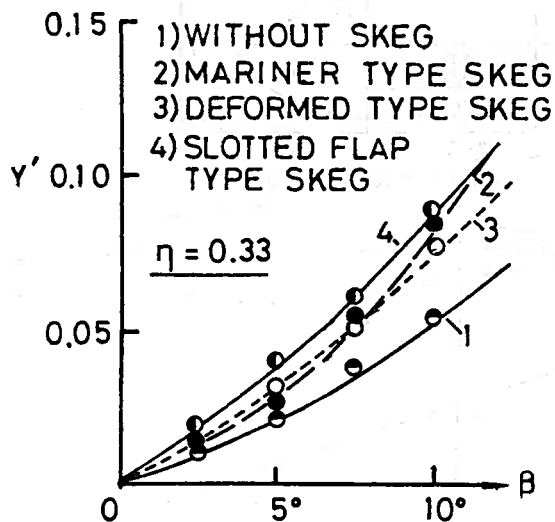


FIG. 7 Lateral Force Acting on Barge

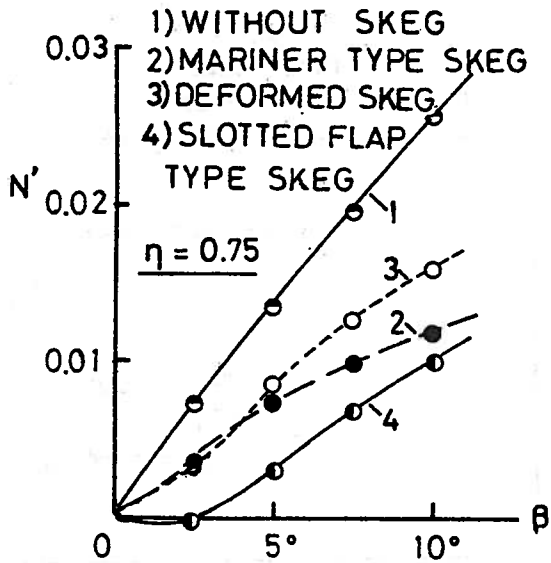


FIG. 8 Yawing Moment Acting on Barge

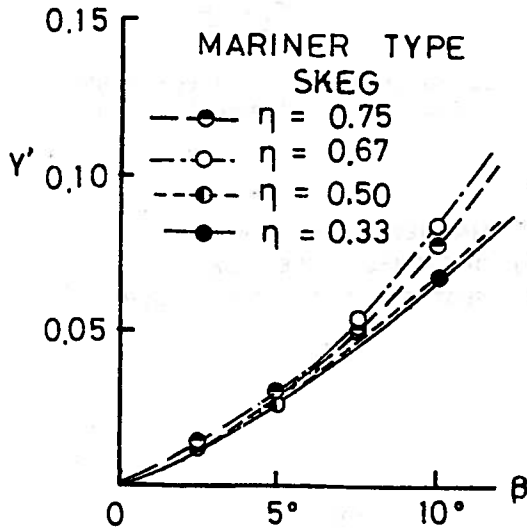


FIG. 9 Lateral Force Acting on Barge

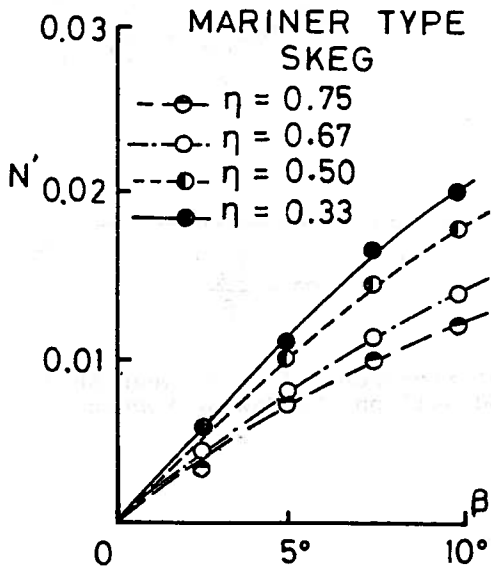


FIG. 10 Yawing Moment Acting on Barge

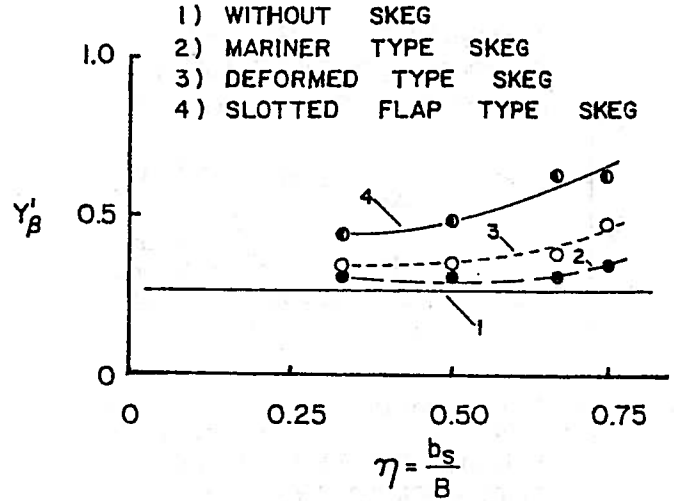


FIG. 11 Static Derivative of Lateral Force Acting on Barge

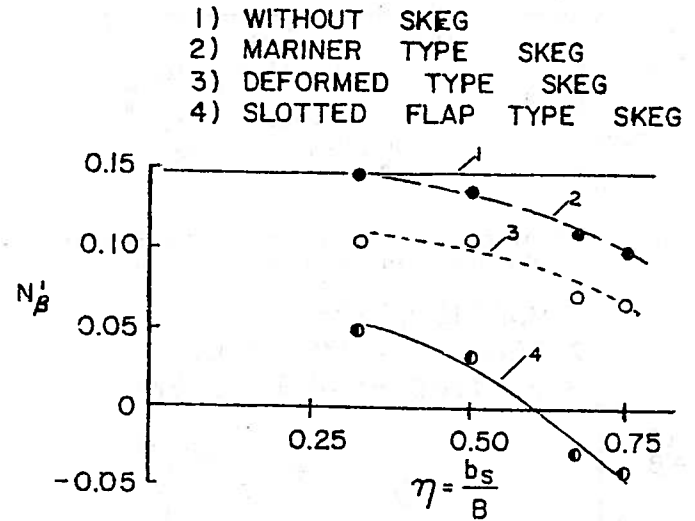


FIG. 12 Static Derivative of Yawing Moment Acting on Barge

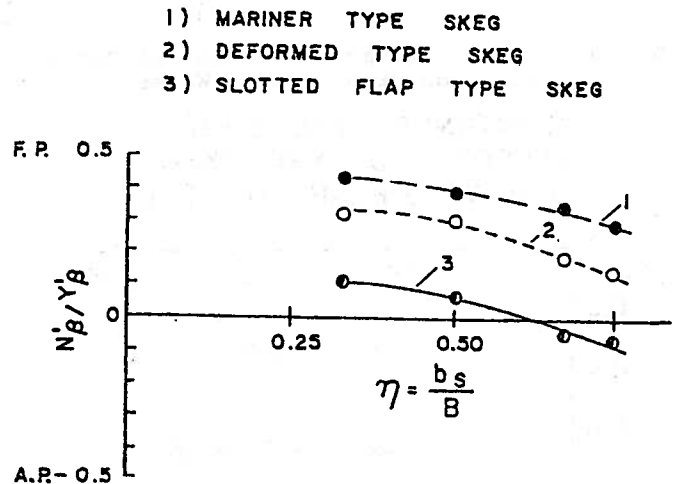


FIG. 13 Center of Action of Lateral Force

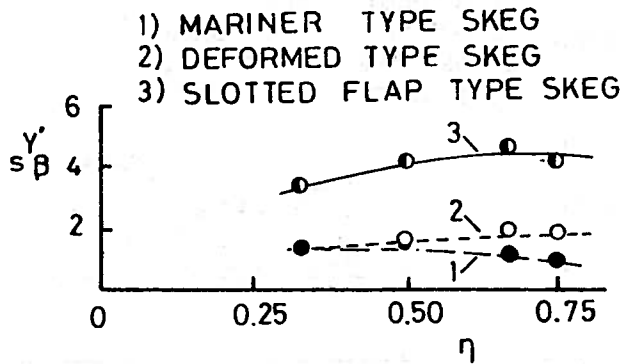


FIG. 14 Static Derivative of Lateral Force Acting on Skeg Behind the Barge Hull

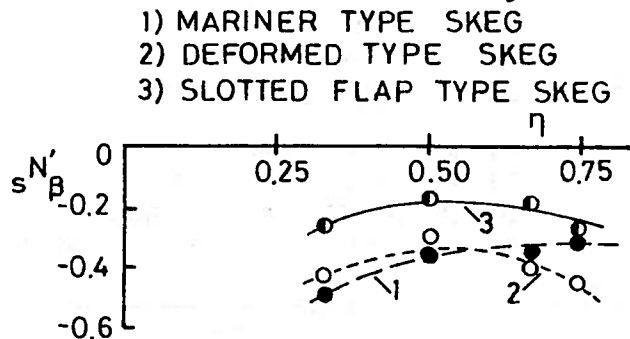


FIG. 15 Static Derivative of Yawing Moment Acting on Skeg Behind the Barge Hull

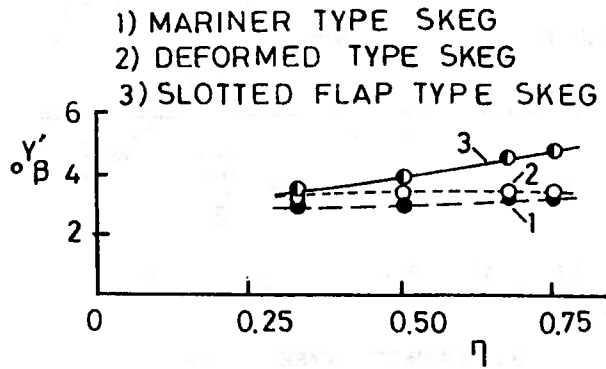


FIG. 16 Static Derivative of Lateral Force Acting on Skeg in Open Water

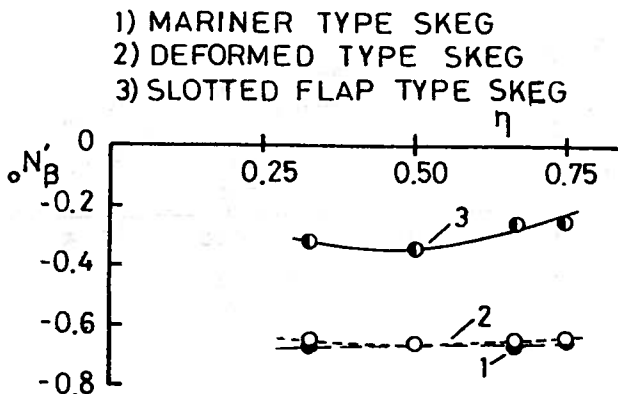


FIG. 17 Static Derivative of Yawing Moment Acting on Skeg in Open Water

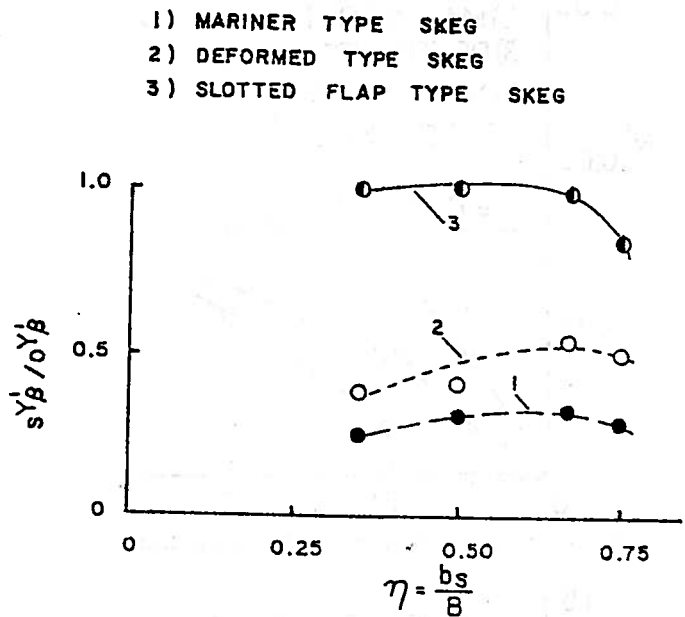


FIG. 18 Interference Effect Between Skeg and Hull on the Lateral Force

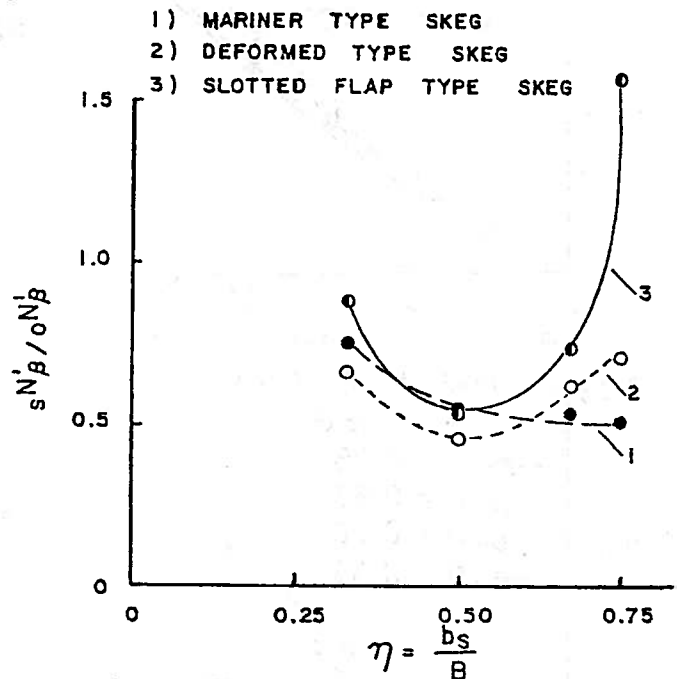


FIG. 19 Interference Effect Between Skeg and Hull on the Yawing Moment

EXPERIMENTAL STUDY ON THE COURSE STABILITY OF A TOWED BARGE¹

BY

M. TANAKA²

ABSTRACT

The ever-increasing demand for barges presents an immediate problem due to the fact that the barge towed by a tug often swings (yaws). This problem is of crucial importance when a towed barge negotiates restricted or congested waters. However the course stability of a towed barge depends on many factors. The method of towing as well as the respective stability of the barge and tug play a significant role. Further, since barges in general have principal dimensions and hull-forms which are different from conventional ships, the estimate of the stability of barge is a formidable problem.

In this paper experimental studies on the course stability of a towed barge are presented, covering two kinds of tests: (i) The respective force and moment acting on a barge and skegs were measured by means of oblique towing test. i.e. the influence of the type of skegs as well as their locations on the stability was clarified. & (ii) Towing tests with systematically varied tow-line and bridle lengths were carried out, and the barge motions were investigated.

The following results relating to the course stability of a towed barge were obtained:

(1) The barge equipped with skegs is more stable than without skegs. The two Slot Skeg is more effective than any other types tested.

(2) It is advisable for the distance between skegs measured with respect to the center line of the barge to be as wide as possible.

(3) The longer the tow-line and bridle lengths are, the more stable the towed barge becomes.

(4) Whether the barge is equipped with skegs or not, the greater the course stability of the barge itself, the more stable the towed barge becomes.

(5) When the tow-line length is fixed, the more stable the barge hull becomes, the shorter the period of motion becomes.

(6) It is generally accepted that the greater the contribution of skegs to the stability is, the more the resistance increases. However, since the skegs tested cause no significant increase of resistance (less than 7%), the use of skegs should be considered from the viewpoint of course stability.

TRANSLATION³

Recently there has been a phenomenal increase in the demand for the transportation of ocean borne construction material by towed barges. With this boom in barge transportation the towing has become a problem.

In the towed condition, there is a chance for the towed vessel to have a large amount of swaying to the right and left. There are many risks that the vessel might disrupt nearby navigation as well as straying outside the limits imposed by the navigation. In addition, the transportation distance is increasing accompanied by barges of larger tonnage. Therefore, the towed barge swaying to the right and left results in meandering which cannot be ignored when the towing distance increases.

The course stability of towed barge vessels does not depend solely on the course stability performance of each barge or towed vessel. Rather it depends on the stability performance of the entire towing system and the method of towing.

In addition, since there are large differences in the main dimensions, bow and stern in comparison with conventional ships, it is difficult to accurately determine, even for individual vessels, the course stability performance from the previously accumulated information.

¹Transactions of the WEST-JAPAN SOCIETY OF NAVAL ARCHITECTS No. 56, August, 1978

²Ishikawajima-Harima Industries, Ltd. Technical Institute

³Prepared by Robert Latorre, Dept. of Naval Architecture and Marine Engineering University of Michigan.

The author made oblique towing tests of a wide beam and shallow draft barge with a cutaway (beveled) bow and stern. This model was used to investigate the effect of fitting skegs to the stern have on the barge form's course stability. The following discusses the investigation of the barge motion as well as the effects observed in systematic tests which varied the skeg design, towrope length, and the bridle length.

2. EXPERIMENTAL MODEL HULL AND SKEGS

The model used in the experiments is shown in Fig.1. Its main particulars are summarized in Table 1. Typically, most barges are designed with a spoon bow and a beveled stern. However, since the speed of the barge used in this study is about 7 knots, which is a relatively low speed, the hull form was derived by simply beveling the bow and stern.

Two skegs used were the same design which Inoue [1] fitted to the stern of a "spoon bow" barge

Table 1 Principal Dimensions of Model Barge

L_{pp} (m)	2,500
B (m)	0.625
d (m)	0.044
C_b	0.97
Δ (kg)	67.5

The four types of skegs used in this investigation had vertical profiles which fitted into the stern cutaway. These skegs are distinguished by their cross sectional profile as follows: Two slot skeg (TSS) which has two slots. One slot skeg (OSS) which has one slot. Mariner Type skeg (MTS) which has a symmetric airfoil section and the Plate Skeg (P.S.) which has a thin flat plate section. The design of the skegs are shown in Figs. 2(a)-2(d). The main particulars of the skegs are summarized in Table 2.

Table 2 Principal Dimensions of Skegs.

Length (m)	0.10
Area (m ²)	0.0024
Area Ratio	1/22.9
Aspect Ratio	0.24

3. TYPES OF EXPERIMENTS AND METHODS

3.1 Oblique Towing Test

The hydrodynamic forces were obtained by oblique towing tests of captive models. An investigation of the effect of skeg form and location on the course stability was made along with a study of the barge course stability without skegs.

The test parameters varied were:

1. Skeg Type, which including the case of no skeg represents five conditions.
2. Drift Angle β , $\beta=15^\circ \sim 0^\circ \sim 15^\circ$
3. Location of Skegs, which consisted of two conditions ($\eta=0.84$ and 0.42) Here when $\eta=0.84$ the skegs are installed at the widest possible spacing.

The notation and coordinate system are shown in Fig. 3.

The barge hull drag force (X), side force (Y) and moment about its center (N) were simultaneously measured with the forces acting on the skegs. These forces were non-dimensionalized using the water density ρ and hull velocity ($U=0.38$ m/s) as expressed below:

$$X' = \frac{X}{\frac{1}{2} \rho L_{pp} d U^2}$$

$$Y' = \frac{Y}{\frac{1}{2} \rho L_{pp} d U^2}$$

$$N' = \frac{N}{\frac{1}{2} \rho L_{pp}^2 d U^2}$$

3.2 Towing Test

In the towing tank tests of the models at an initial displacement, the barge model is restrained by a clamp at an approximate offset of $1.6 \times B$. When the towing carriage reached a constant speed, the model was released and measurements were made of the towrope tension, angle, as well as the barge's turning angle and angular velocity. There was special concern to avoid having the measurement chord influence the motions of the model. Therefore, a small gyro and batteries were installed and during the tests the data was transmitted to the towing carriage by using radio telemeter. Thus the only connection between the carriage and models was the piano wire used for the towrope. These offset towing tests were made at a constant .38m/s speed while systematically varying the towrope length L and bridle length ℓ as described below:

- 1) Towrope length L , $L=L_{pp}$, $2L_{pp}$, $3L_{pp}$
- 2) Bridle length ℓ , $\ell=0$, $0.1 L_{pp}$, $0.2 L_{pp}$, $0.3 L_{pp}$ where L and ℓ are defined as shown in Fig.4.

When the model is towed by a towing carriage, the tests correspond to towing with an extremely large towing vessel

		Y'_β	N'_β	N'_β/Y'_β	$\frac{A}{L_{pp} \cdot d} L'_\beta$
	Without Skegs	0.386	0.058	0.150	-
$\eta = 0.84$	Two Slot Type Skeg (TSS)	0.502	0.027	0.054	0.074
	One Slot Type Skeg (OSS)	0.478	0.041	0.086	0.025
	Mariner Type Skeg (MTS)	0.393	0.084	0.214	-
	Plate Type Skeg (PS)	0.421	0.068	0.162	-
$\eta = 0.42$	Two Slot Type Skeg (TSS)	0.449	0.047	0.105	0.025
	One Slot Type Skeg (OSS)	0.386	0.056	0.145	0.014
	Mariner Type Skeg (MTS)	0.295	0.072	0.244	-
	Plate Type Skeg (PS)	0.263	0.080	0.304	-

TABLE 3 Derivatives

There is a towing method [2] using a model towing ship which nearly corresponds to the actual towing conditions. However due to the difficulties in the measurements and the towing tank width limitations, this method was not used and the experiments were made using the towing carriage.

In these towing tests the spacing between the skegs was set at $\eta = 0.84$.

4. RESULTS OF EXPERIMENTS

4.1 Results of Oblique Towing Tests

The influence of the skegs on the barge hydrodynamic derivatives will be discussed. The notation adopted is mainly taken from the text of the Second Maneuvering Symposium [3]. The derivatives of the barge hull without the skegs are denoted by "o" and written as: ${}^o Y'_\beta$, ${}^o N'_\beta$, ${}^o Y'_r$, and ${}^o N'_r$.

Ignoring the interference between the hull and skegs, the derivatives of the barge hull with skegs are written:

$$\begin{aligned}
 Y'_\beta &= {}^o Y'_\beta + \frac{A}{L_{pp} \cdot d} L'_\beta \\
 N'_\beta &= {}^o N'_\beta - \frac{A}{L_{pp} \cdot d} \frac{\ell_s}{L_{pp}} L'_\beta \\
 Y'_r &= {}^o Y'_r + \frac{A}{L_{pp} \cdot d} \frac{\ell_s}{L_{pp}} L'_\beta \\
 N'_r &= {}^o N'_r - \frac{A}{L_{pp} \cdot d} \left(\frac{\ell_s}{L_{pp}} \right)^2 L'_\beta
 \end{aligned} \quad (1)$$

where:

ℓ_s : The distance from Φ to the skeg position

Here $\frac{\ell_s}{L_{pp}} \doteq 0.5$

A : Projected area of the vertical skeg cross section

The second term on the right hand side of equation (1) expresses the influence of the skegs on the hydrodynamic derivatives. Considering that the term $\frac{A}{L_{pp} \cdot d} L'_\beta$ adds a value of 1 to Y'_β , the corresponding increase in the value of N'_β and Y'_r is 0.5, and the corresponding increase to N'_r is 0.25.

Consequently, there is a large effect from installing the skegs on the value of Y'_β followed by N'_β and Y'_r . This was also found in the previously reported results of Inoue [1] and Takekawa [4]. Therefore it is possible to determine the optimum skeg by oblique towing tests of captive models.

The course stability of a vessel is indicated by the Δ index.

$$\Delta = Y'_r - (m' + m'_x) N'_\beta - N'_r Y'_\beta \quad (2)$$

Substituting (1) into (2), the effect of the skegs on the hull course stability is as follows:

$$\begin{aligned}
 \Delta &\doteq \Delta_o + \frac{A}{L_{pp} \cdot d} L'_\beta \left[\frac{\ell_s}{L_{pp}} {}^o N'_\beta - \right. \\
 &\quad \left. - \frac{\ell_s}{L_{pp}} ({}^o Y'_r - (m' + m'_x) - {}^o N'_r) \right] \quad (3)
 \end{aligned}$$

Since the value of the terms inside the brackets [] is usually positive, there will be an improvement in the barge course stability when the skegs with a value of $L'_\beta > 0.0$ are installed behind the hull's center of gravity. There will be a phenomenal improvement when L'_β is large.

Comparing the derivative values for the barge with and without the skegs, when the skegs are present the Y'_β values increase while the value of N'_β decreases so N'_β/Y'_β , the location of the center of pressure moves backward.

While the course stability is improved by the four types of skegs, the best course stability is obtained by the TSS followed by the OSS. In comparison with these skegs the MTS and PS skegs cause only a small improvement. These experimental results are the same as those obtained by Inoue [1] for a barge model with a spoon bow.

It was found that while the course stability performance improves when $\eta = 0.84$, when $\eta = 0.42$, there is little difference in the course stability performance with and without the skegs. Usually when foils are arranged in a line their performance characteristic is different due to the influence

of adjacent foils. When skegs are fitted to a barge they are arranged symmetrically along the hull centerline. When the separation distance becomes small an effect similar to the one observed for foils in a straight line occurs and the resulting lift force of the skeg decreases.

Therefore a large improvement in the course stability performance can be obtained by installing skegs which generate high lift forces. The skeg locations should be as far as possible behind the center of gravity of the hull and the separation distance should be as wide as possible.

4.2 TOWING TEST RESULTS

The aft clamp was released when the towing carriage reached a constant speed. Then after an interval of time, the displacement of the barge from the tank centerline would decrease. However the barge motion was extremely large when its initial displacement was about $1.6 \times B$ when the aft clamp was released.

In these tests while there was a decrease in the barge motion with time, during the towing tests the data indicated that the barge was course unstable for very small motions. It thus became clear that the decrease in the motion is due to the large initial displacement.

The following two coefficients were adopted to treat this decrease in motion:

The first is a dissipation coefficient. Here a technique of analysis similar to that used in free rolling experiments is utilized. Using the dissipation curve of the turning angle θ , the coefficient M is shown in Figs. 5(a)-5(b) was obtained.

$$\Delta\theta = M \cdot \theta_m^2 \quad (4)$$

The second is the coefficient of the time average of the turning angle $|\dot{\theta}|_{avg}$. This coefficient is related to the damping motion.

$$|\dot{\theta}|_{avg} = \frac{1}{\theta_0 T} \int_0^T |\dot{\theta}| dt \quad (5)$$

where at $t = 0$, $\theta = \theta_0$

The time average coefficient is shown in Figs. 6(a)-6(b).

The following treats the damping of the motion during towing in order to study the influence of the skeg type, towrope length, and bridle length on the barge course stability. In other words, the course stability performance is good when there is a strong damping of the barge motion. This occurs when the coefficient M in expression(4) has a large value and when the value of $|\dot{\theta}|_{avg}$ in expression(5) is small.

Therefore in this discussion the turning angle analysis is presented using the coefficients described earlier. The other items measured in the tests will not be discussed except for the towrope tension.

4.2.1 Effect of Towrope Length, L

Figs. 5(a) and 6(a) show the trends in the coefficients M and $|\dot{\theta}|_{avg}$ with different lengths of towrope L . When the towrope length is large there is a strong damping of the motion and the course stability performance is good. The coefficients do not appear to have a linear relationship with the towrope length L . For example in Fig. 5(a) for $\ell/Lpp = 0$, the results for the two slot skeg (TSS) indicate that when the value of $L = 3Lpp$, there is a drop off in the increase of M . In Fig. 6(a) for $\ell/Lpp = 0$, the value of $|\dot{\theta}|_{avg}$ for the two slot skeg (TSS) at $L = 2Lpp$ indicates better course stability performance than at $L = 3Lpp$. It appears that a large improvement in the barge course stability will not be obtained when larger values of L are used.

This figure also indicates that when the original course stability performance is poor there will be hardly any improvement from increasing the value of L/Lpp when the value of ℓ/Lpp is small.

4.2.2 Effect of Towing Bridle Length, ℓ

With the exception of $L = 3Lpp$, it appears from examining Fig. 5(b) that there is a linear relationship of the coefficient M with the value of ℓ . In the case of $L = 3Lpp$ the coefficient M has its largest value when $\ell = 0.1Lpp$. This tendency is especially pronounced for the two slot skeg (TSS) and one slot skeg (OSS) whose course stability performance indicated by M appear to be as good as the barge itself. It should be also noted that with these skegs (TSS and OSS) the course stability performance is better at $\ell = 0.1Lpp$ than at $\ell = 0.3Lpp$.

The barge course stability performance becomes extremely good when either the TSS or OSS skegs are fitted. This was previously observed in the inclined towing test results. Consequently even when towing at a towrope length of $L = 3Lpp$, the course stability performance of the barge with these skegs is very good. In these tests at $L = 3Lpp$ when the clamp was released the motion was so damped as to become periodic. In this situation the expression for M becomes meaningless.

From the values of $|\dot{\theta}|_{avg}$ shown in Fig. 6(b) it appears that there is an inverse relationship between the bridle length ℓ and $|\dot{\theta}|_{avg}$. Thus $|\dot{\theta}|_{avg}$ becomes small when the towing bridle length ℓ becomes large and the course stability performance improves

The turning angle θ was also assumed to have the following governing equation:

$$\theta = \theta_0 \cdot e^{-\frac{t}{T_D}} \quad (6)$$

The time constant T_D is shown in Fig. 7. This constant exhibits the same trends as $|\dot{\theta}|_{\text{avg}}$.

4.2.3 Influence of Barge Hull on the Course Stability Performance

Figs. 5(a), 5(b), 6(a), 6(b), and 7 indicate that the differences in the towing course stability seem to have the same trends as the barge without skegs. It can be expected that a course stable barge hull form will have good course stability when it is towed.

It has been pointed out that the course stability in towing improves when longer towrope and towing bridle lengths are used. However, since there are limits to these lengths imposed by towed barge's turning performance as well as its interaction with other vessels, it is not expected that there will be further improvements from using longer towrope and bridle lengths.

While it is desirable that the hull form design has good course stability performance, if the barge's course stability is in question then it is advisable to improve the course stability by using a suitable skeg design.

4.2.4 Period of Barge Motion

The relation between the towing bridle length ℓ and the average period of the barge motion T_m is shown in Fig. 8. The barge has good course stability performance when the value of ℓ increases and the value of T_m is small. Assuming that the towed barge system can be modeled as a pendulum the length of the pendulum's string corresponds to the towrope length L . The natural period of the system is then related to \sqrt{L} and the damping force acting on the system is related to the skeg type and the towing bridle length ℓ . Thus the motion becomes small as L becomes large and the value of T_m increases.

4.2.5 Relationship of Skegs to Resistance

The average tension force during the towing tests is shown in Fig. 9 for $L = 2L_{pp}$ and $L = 3L_{pp}$. For each type of skeg these values are constant irrespective of L and ℓ . The largest tension forces were measured for the two slot skegs (TSS) and the one slot skegs (OSS). The average value of tension force representing the hull resistance can be divided into two groups. It appears the skegs in addition to improving the barge course stability performance, cause a noticeable increase in the barge's towing resistance.

Consequently it is necessary when designing the skeg to consider in addition to the improvement in course stability, the resulting overall resistance necessary to obtain a course stable barge. In this study there is not an exceptionally large increase in the resistance from installing the skegs. The maximum resistance increase is 7%. Thus the most suitable skeg for this barge design is the two slot skeg (TSS) since the course stability improvement is large and its resistance increase is small.

5. CONCLUSIONS

A course stability performance investigation was made for a wide beam, shallow draft barge model tested in a towing tank.

It was shown that oblique towing tests were useful in investigating the effect of skegs on the barge hull's hydrodynamic derivatives. The influence of skeg type and skeg spacing on the barge course stability performance was investigated using four types of skegs and the oblique towing technique.

Systematic towing tank tests were also conducted to determine the influence of skeg type, towrope length, and towing bridle length on the barge course stability performance.

The phenomenon of the damping in the barge motion was characterized by two coefficients M and $|\dot{\theta}|_{\text{avg}}$. The course stability performance was considered good when the barge motion exhibited large damping.

The following summarizes the conclusions obtained in these studies.

- 1.) It is possible to improve the course stability performance by installing skegs. Among the skegs used in the tests, it was shown that the two slot skeg (TSS) was very effective.
- 2.) It is best to use as wide a separation width between the skegs as possible.
- 3.) Towing with longer towrope and towing bridle lengths resulted in improved course stability performance.
- 4.) The better the barge course stability performance without skegs, the better its course stability will be in towing.
- 5.) In the case of constant towrope length the course stability performance is good when the radius of the barge motion is small. Keeping the other parameters constant and letting the towrope length become longer, the course stability performance will improve and the period of the motion will be longer.
- 6.) The larger the skegs contribution to improving the barge course stability performance, the stronger the damping of the barge motion and the larger the increase in the barge resistance. In the present

study the resistance increase was within 7% so consideration was given exclusively to the selection of skegs to improve the course stability performance.

The author would like to express his sincere thanks to Professors S. Inoue, and K. Kijima of Kyushu University for their valuable advice during this study.

The oblique towing tank tests were completed in the seakeeping and maneuvering tank of Kyushu University. The towing tests were made at the experimental model basin of the Research Institute of Ishikawajima-Harima Industries, (IHI), Ltd.

The author is deeply grateful to chief engineer Dr. T. Jinnaka and manager Mr. M. Nanimatsu of IHI for their valuable advice and encouragement during this study. Thanks are also extended to Dr. Tasaki and the staff of the IHI experimental tank for their cooperation in carrying out the experiments. The author is especially thankful to Mr. Sekine for his help in carrying out the towing tests.

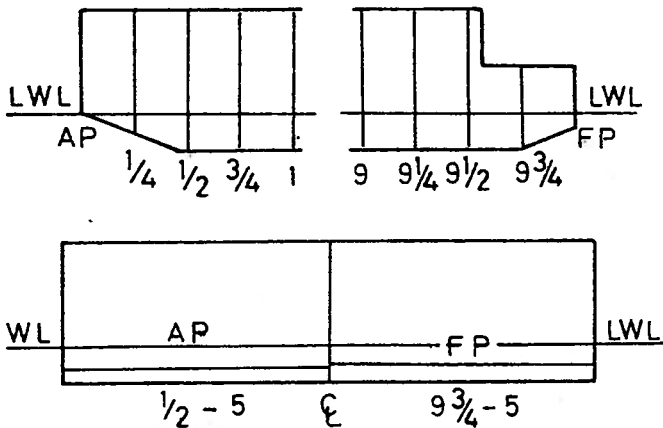


FIG. 1 Lines of Barge Model

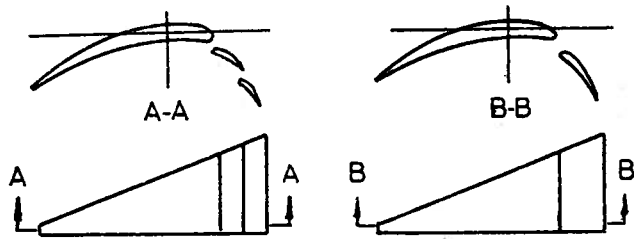


FIG. 2(a) Two Slot Skeg (TSS)

FIG. 2(b) One Slot Skeg (OSS)

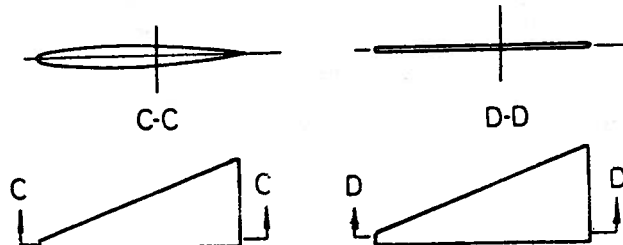


FIG. 2(c) Mariner Type Skeg (MTS)

FIG. 2(d) Plate Skeg (PS)

LITERATURE

1. Inoue, S., et. al., "On the Course Stability of a Barge," TRANSACTIONS OF WEST-JAPAN SOCIETY OF NAVAL ARCHITECTS, No. 54, August, 1977, pp. 193-201. (In Japanese) TRANSLATION: Improving Barge Towing translation No. B-I-3, R. Latorre.
 2. Inoue, S., et. al., "Some Studies of Towed Ships System," TRANSACTIONS OF WEST-JAPAN SOCIETY OF NAVAL ARCHITECTS, No. 50, August, 1975, pp. 65-74. (In Japanese) TRANSLATION: Improving Barge Towing Translation No. B-I-2, R. Latorre.
 3. Second Manoeurability Symposium, SOCIETY OF NAVAL ARCHITECTS OF JAPAN, 1970, (In Japanese)
 4. Takekawa, M., et. al., "Course Stability of Towed Large Barge," JOURNAL OF THE SOCIETY OF THE NAVAL ARCHITECTS OF JAPAN, Vol. 137, June, 1975, pp 186-195, (In Japanese)
- ALSO: Nagamatsu, S. et. al., "Reports on Tank Tests and Full Scale Ship Experiment for Lash Feeder Barge," JAPAN SHIPBUILDING AND MARINE ENGINEERING, Vol. 11, No. 2, 1979.

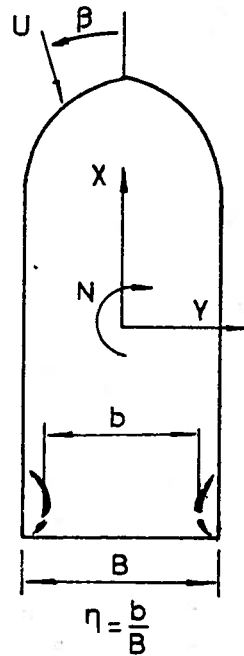


FIG. 3 Coordinate System

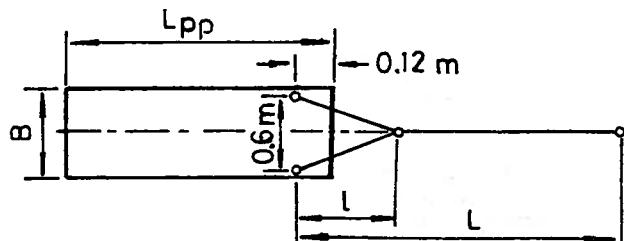


FIG. 4 Definition of l and l

KEY (FIGS. 5-9)

- WITHOUT SKEGS
- △—△ TWO SLOT SKEGS
- ONE SLOT SKEGS
- x—x MAINER TYPE SKEGS
- ▽—▽ PLATE TYPE SKEGS

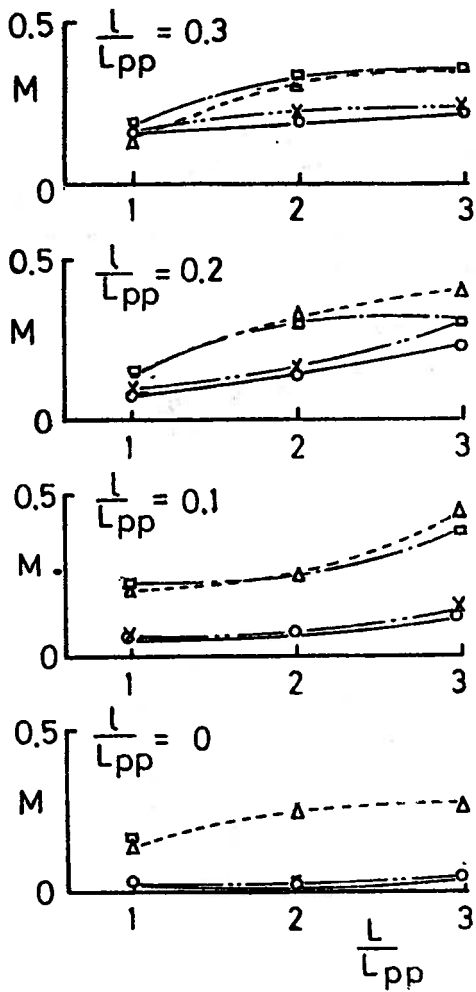


FIG. 5(a) Extinction Coefficient (M)

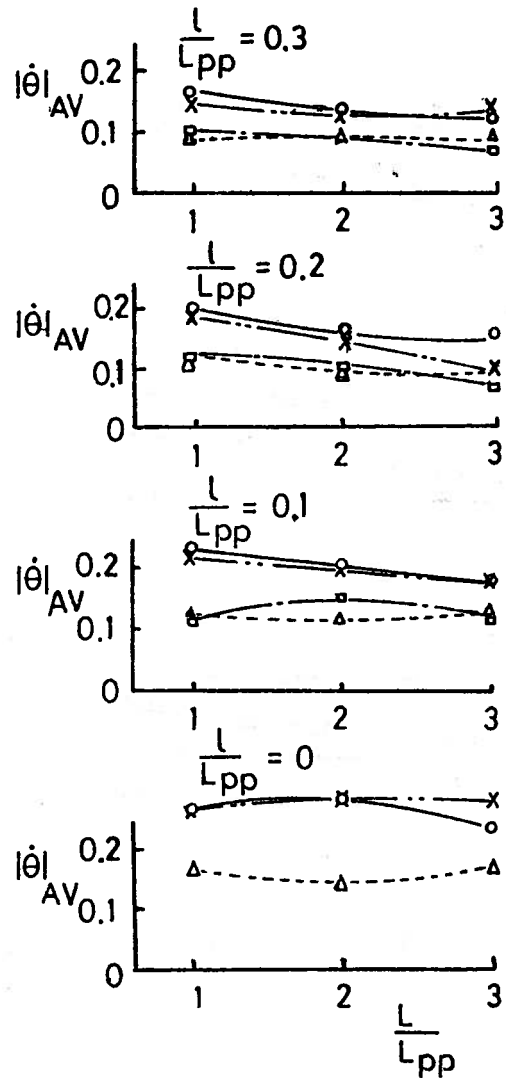


FIG. 6(a) Time Average $|\dot{\theta}|_{avg}$

KEY (FIGS. 5-9)

- WITHOUT SKEGS
- △—△ TWO SLOT SKEGS
- ONE SLOT SKEGS
- x—x MAINER TYPE SKEGS
- ▽—▽ PLATE TYPE SKEGS

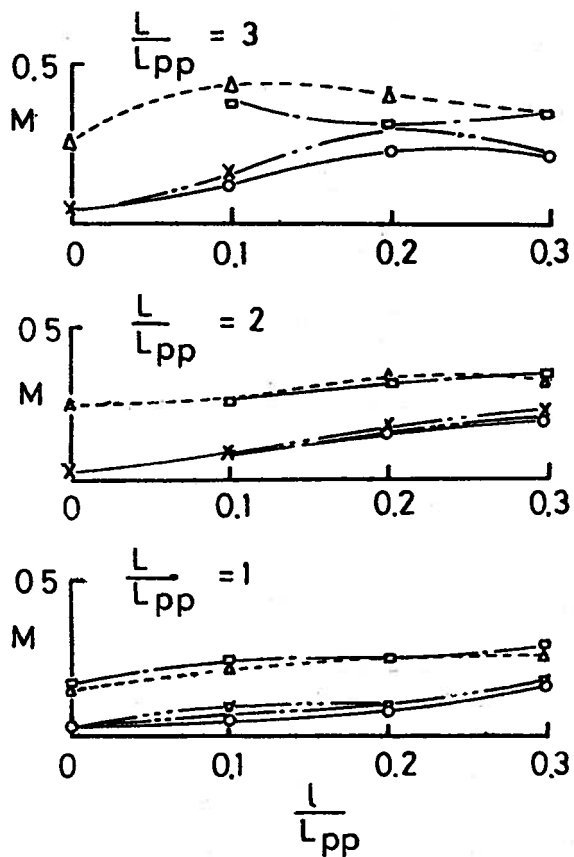


FIG. 5(b) Extinction Coefficient (M)

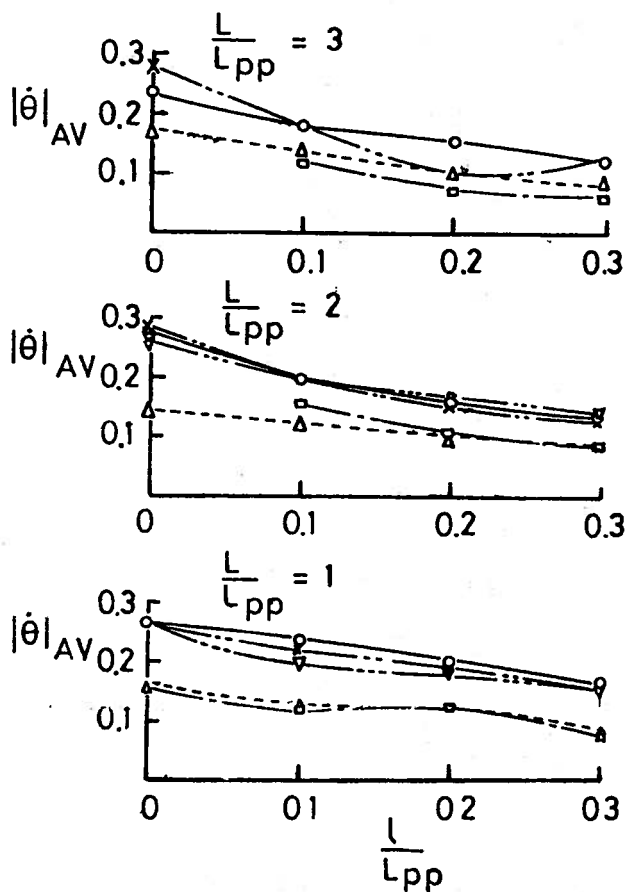


FIG. 6(b) Time Average $|\dot{\theta}|_{avg}$

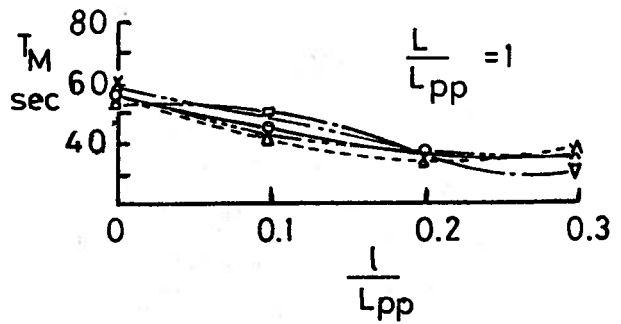
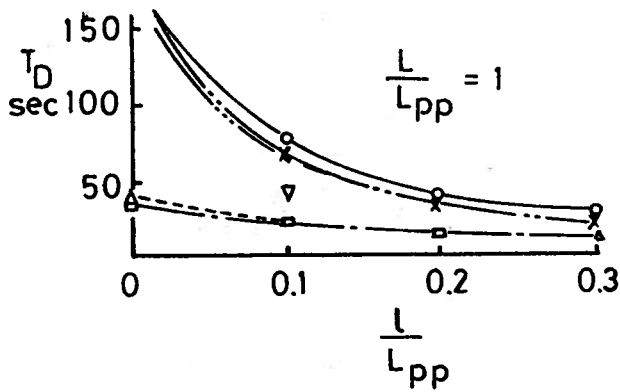
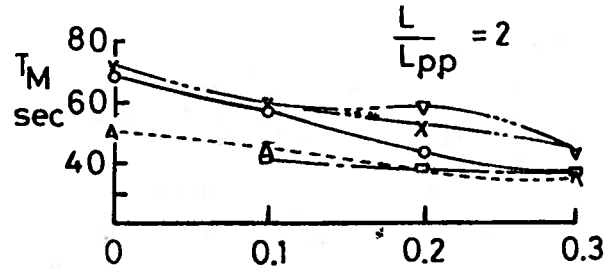
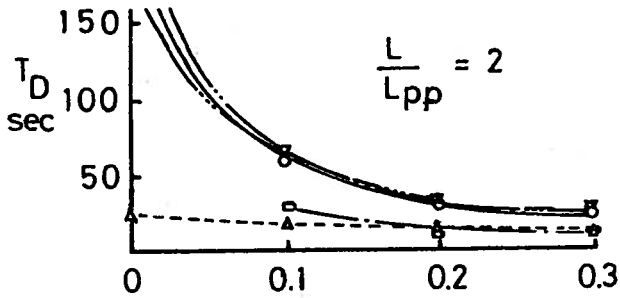
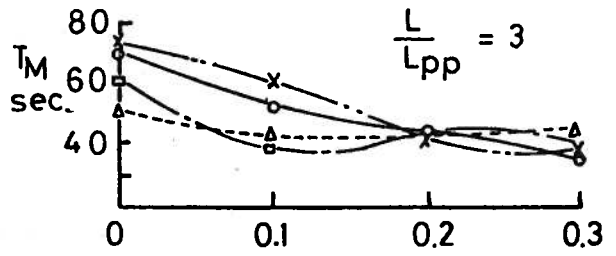
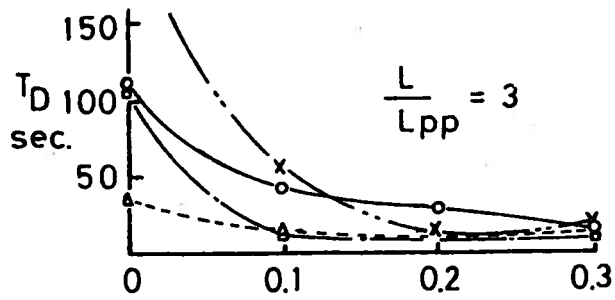


FIG. 7 T_D

FIG. 8 Mean Period (T_m)

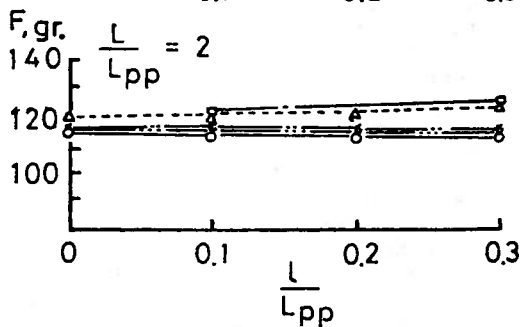
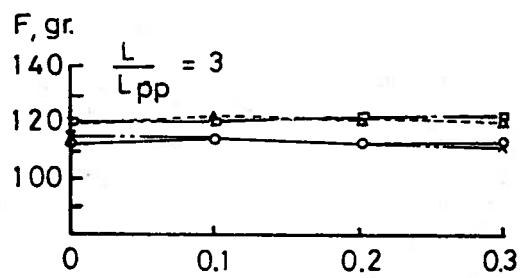


FIG. 9 Mean Towing Force (F)

ANALYSIS OF THE SPONTANEOUS YAWING OF TOWED SHIPS¹

BY

E.B. YUDEN
A.G. MIKOVSKY

SUMMARY

This paper presents a theoretical analysis of ship motion during towing. The authors treat the phenomenon of spontaneous periodic yawing and the influence the various design variables have on this yawing. The equations of motion are reduced to a characteristic equation to define the limits of stable towing. The frequency of the oscillation and the effect of the bridle on towing are also examined [Translator].

TRANSLATION²

In ocean navigation there often arises a period during which it is necessary to tow a single ship. This problem and its related points have been dealt with for a long time [1-6]. With the recent level of theoretical development and experimental facilities, it is now possible to obtain the data required for constructing an accurate mathematical description of the towing process for actual vessels. In this case, the utilization of an electric computer makes it possible to readily reproduce the towing process itself and analyze each component.

Presently we are concerned with the development of a general formulation which includes special features of the towing process to allow their inclusion to obtain a practical solution. Among the features not examined earlier is the phenomenon observed during towing, even in the absence of sea waves and wind, of the spontaneous periodic yawing of the towed ship having characteristic free oscillations. Since in practice this oscillatory state should be avoided during towing, it is necessary to understand the conditions determining the onset of the oscillations and to estimate the dependence of their parameters (design) on the conditioning factors. The investigation indicates that the basic results can be obtained within the limits of the traditional assumptions used in characterizing the response of the towing system. These are, namely, that during towing the distance measured as a straight line between the attachment points of the cables connecting the towed ships remains constant during towing and the motion takes place in calm water. Furthermore,

assuming that the towing speed is constant, the angle parameters determining the relative position of ships fluctuate in such limits that the sine of the angle can be replaced by the angle itself and its cosine by unity.

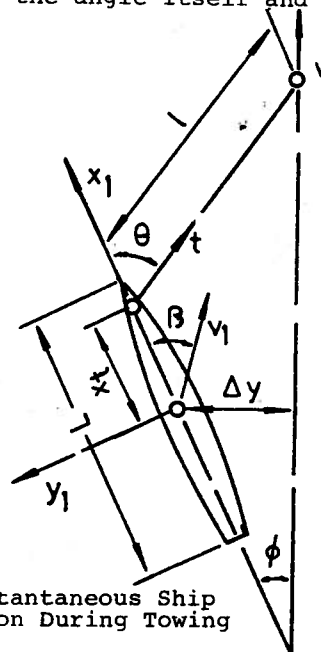


Fig. 1 Instantaneous Ship Position During Towing

Fig. 1 shows the basic notation for the geometrical and kinematic quantities encountered below. The following equality can be obtained from considering this figure:

$$\theta = \frac{\Delta y}{L} + \phi \left(1 + \frac{x_t}{L}\right) \quad (1)$$

$$\frac{d\Delta y}{dt} = -v(\beta - \phi) \approx v(\phi - \beta)$$

Introducing the notation:

$$p = \frac{d}{dt} \quad \text{Differential Operator}$$

$$\tau = t \frac{v}{L} \quad \text{Non dimensional time}$$

¹ Sudostroyeniye, No. 4, April, 1975, pp. 15-17.

² Prepared by R. Latorre, Dept. of Naval Arch. & Mar. Eng., Univ. of Michigan.

$\kappa = \frac{S \cdot L}{V}$ Scale Factor
 S Area of the immersed part of the hull centerplane
 V Volume of ship's displacement
 $C_T = \frac{T}{\rho/2u^2 S}$ Thrust coefficient (Towing Force Coefficient)
 C_1, C_2, m_1, m_2 Hydrodynamic Coefficients
 k_{11}, k_{33}, k_{55} Coefficient of added mass
 \bar{r} Non-dimensional rotational inertia of ship relative to Z axis
 $\bar{x}_t = \frac{x_t}{L}$, Relative values of the distance x_T and L
 $\bar{\ell} = \frac{\ell}{L}$

Following the work [7], the equation of motion for the towed ship taking into account the assumed notation and relation (1) with absence of disturbing forces will assume the form of:

$$2(1 + k_{33})p\beta - 2(1 + k_{11})p\phi + K(C_1\beta + C_2|\beta|\beta) = KC_T\theta$$

$$-2\bar{r}^2(1 + k_{55})p^2\phi - km_3p\phi + km_1\beta = k\bar{x} \cdot C_T\theta \quad (2)$$

$$p\theta = \frac{1}{\bar{\ell}}(\phi - \beta) + (1 + \frac{\bar{x}_t}{\bar{\ell}})p\phi$$

Following reference [7], we introduce the additional notation:

$$\begin{aligned}
 q_{21} &= \frac{KC_1}{2(1+k_{33})} ; & q_{31} &= \frac{Km_1}{2\bar{r}^2(1+k_{55})} \\
 h_1 &= \frac{KC_2}{2(1+k_{33})} ; & r_{31} &= \frac{Km_3}{2\bar{r}^2(1+k_{55})} \\
 r_{21} &= \frac{1+k_{11}}{1+k_{33}} ; & s_{31} &= \frac{K\bar{x}_t C_T}{2\bar{r}^2(1+k_{55})} \\
 s_{21} &= \frac{KC_T}{2(1+k_{33})}
 \end{aligned} \quad (3)$$

$$q = q_{21}r_{31} - q_{31}r_{21}$$

$$\bar{s} = q_{21}r_{31} - q_{31}s_{21}$$

$$s = r_{21}s_{31} - r_{31}s_{21}$$

$$\bar{x}_\beta = \frac{m_1\beta}{C_1\beta + C_2|\beta|\beta}$$

$$\bar{x}'_\beta = \frac{m_1}{C_1 + 2C_2|\beta|}$$

$$\bar{x}_{p\phi} = \frac{Km_3p\phi}{2(1+k_{11})p\phi}$$

where \bar{x}_β Position of the relative arm of the hydrodynamic force (center of pressure)

\bar{x}'_β Ratio of derivative of drift angle position moment to position hydrodynamic force

$\bar{x}_{\beta\phi}$ Relative arm of damping force.

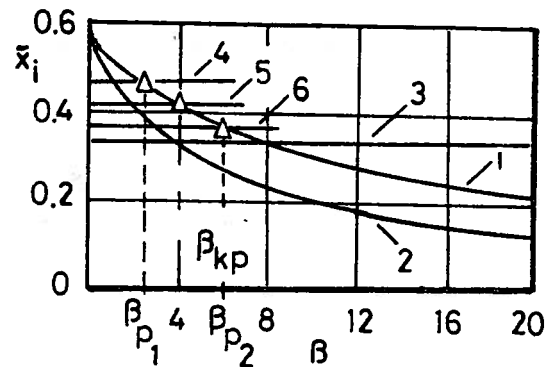


FIG. 2 Characteristic Relation of Hydrodynamic Arm with Drift Angle

Key: 1. \bar{x}_β , 2. \bar{x}'_β , 3. $\bar{x}_{p\phi}$
 4. \bar{x}_t corresponding to unstable equilibrium
 5. $\bar{x}_t = \bar{x}_{t2}$
 6. \bar{x}'_β corresponding to stable equilibrium

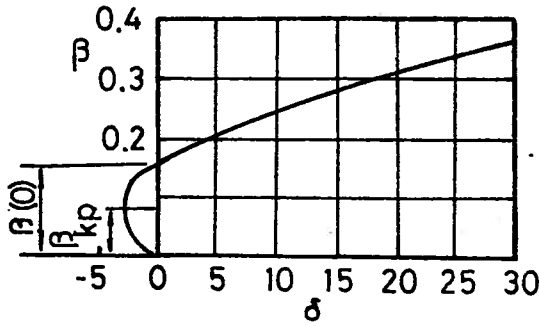


Fig. 3 Dependence of Ship Drift Angle in Steady Turn by Moving the Rudder

$$\beta(0) = -\frac{q}{n_1 r_{31}} ; \beta_{kp} = -\frac{q}{2h_1 r_{31}}$$

The characteristic dependence of the values of \bar{x}_β , \bar{x}'_β and $\bar{x}_{p\phi}$ on the drift angle for an unstable ship is illustrated in Fig. 2. The maneuvering diagram characteristic for this example ship is presented in Fig. 3.

The initial consideration is given to the possible equilibrium state of the system described by equation (2). Assuming that $p=0$ and designating the equilibrium values of β as β_p , we obtain the following equation for determining the equilibrium from the basic equations (2), (3) and (4)

$$(\bar{s} + s_{31} h_1 \beta_p) \beta_p = 0$$

Here two cases are possible (see Fig. 4 and curve 1 in Fig. 5)

1) $\bar{s} > 0 ; \beta_p = 0$

2) $\bar{s} < 0 ; (\bar{s} + \bar{s}_{31} h_1 \beta_p) = 0 ; \beta_p = -\frac{\bar{s}}{s_{31} h_1}$

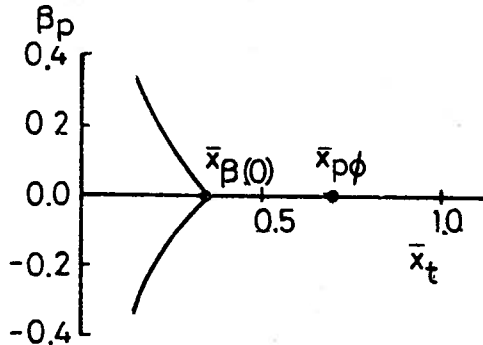


Fig. 4 Dependence of the drift angle in equilibrium position on the location of towing cable fastening point for a nonasymptotically stable ship.

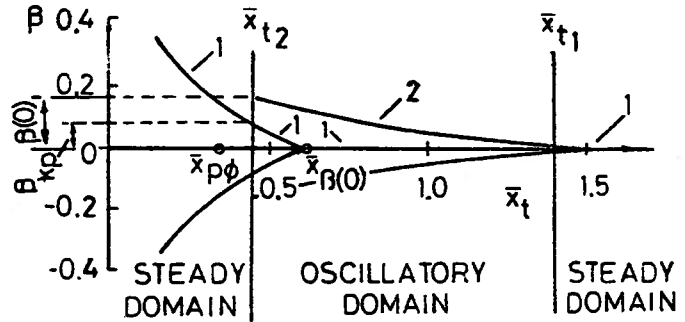


Fig. 5 Possible drift angle values for towing unstable ship

- 1 β_p Characteristic equilibrium position
- 2 β_o Amplitude of oscillation

The first case corresponds to the conditions $\bar{x}_t > \bar{x}_\beta(0)$. This means that the cable fastening point is displaced towards the bow from the center of pressure acting on the hull at zero drift angle. The second case corresponds to the conditions of $\bar{x}_t < \bar{x}_\beta(0)$. In this case $\bar{x}_\beta(\beta_p) = \bar{x}_t$, that is the center of pressure for $\beta = \beta_p$ coincides with the \bar{x}_t abscissa.

Returning now to the analysis of stability we consider the equilibrium position and use the equation of motions describing a disturbance relative to the equilibrium position.

Analysis indicates that after the disturbance the motion will be stable or unstable depending firstly if:

$$\bar{x}_{p\phi} + \bar{x}_t \frac{s_{21}}{r_{21}(q_{21} + 2h_1 \beta_p)} - \bar{x}'_\beta(\beta_p) > 0 \quad (7)$$

To find the value of the arm \bar{x}_t , which enables the inequality (7) to be transformed to the equation:

$$\bar{x}_{p\phi} + \bar{x}_t \frac{s_{21}}{r_{21}(q_{21} + 2h_1 \beta_p)} = \bar{x}'_\beta(\beta_p) \quad (8)$$

Here again we have two cases:

$$\beta_p = 0 \quad (9)$$

$$\beta_p = -\frac{\bar{s}}{s_{31} h_1} = -\frac{q_{21}}{\bar{x}_t h_1} [\bar{x}_t - \bar{x}_\beta(0)]$$

In the first case, taking into account that $\bar{x}_\beta(0) = \bar{x}_\beta(0)$ results in

$$\bar{x}_t = \frac{r_{21}q_{21}}{s_{21}} [\bar{x}_\beta(0) - \bar{x}_{\rho\phi}]$$

and for the second case:

$$\bar{x}_t = \frac{2\bar{x}_\beta(0)\bar{x}_{\rho\phi}}{\bar{x}_\beta(0) + \bar{x}_{\rho\phi}}$$

In this manner, it can be confirmed that the necessary conditions for stable motion occurs when:

$$\bar{x}_t < \bar{x}_{t_2}$$

$$\bar{x}_t < \bar{x}_{t_1}$$

and that in the range $\bar{x}_{t_1} < \bar{x}_t \leq \bar{x}_{t_2}$

the disturbing motion will become unstable (lead to unstable motion).

In the latter case, the parameter β is nonlinear due to the oscillation. Assuming that in the state of oscillation, $\beta = \beta_0 \sin \bar{v}t$ and adopting harmonic linearization of the nonlinear component $h_1 |\beta| \beta$ results in:

$$h_1 |\beta| \beta \cong \frac{8}{3\pi} h_1 \beta_0 \beta = h_1^* \beta_0 \beta \quad (10)$$

Taking into account equations (3), (4) and (10), the system of equations (2) can be reduced to the following differential equation relative to the variable β :

$$\left\{ p^4 + (r_{31} + q_{21} + h_1^* \beta_0) p^3 + [q + r_{31} h_1^* \beta_0 + s_{31} + \frac{1}{\bar{x}} (s_{21} + \bar{x} s_{31})] p^2 + \left[(1 + \frac{x_t}{\bar{x}}) \bar{s} + s_{31} h_1^* \beta_0 + \frac{1}{\bar{x}} (s_{31} - \bar{s}) \right] p + \frac{1}{\bar{x}} (\bar{s} + s_{31} h_1^* \beta_0) \right\} \beta = 0 \quad (11)$$

The characteristic equation corresponding to expression (11) has the form

$$p^4 + a_1 p^3 + a_2 p^2 + a_3 p + a_4 = 0 \quad (12)$$

where the values of the coefficients a_1 , a_2 , a_3 and a_4 are clear from comparing

equations (11) and (12). Assuming $p = i\bar{v}$ and substituting it into equations (12) results in an equation for determining the amplitude β_0 and frequency \bar{v} .

Numerical analysis indicates that for cable lengths $l > 3$ and values of $x_t < 0.5$, the terms containing the factor $1/\bar{x}$ become insignificant. This permits investigating a simplified equation instead of equation (11) and the solution gives the following results.

$$\beta_0 = - \frac{q}{h_1^* r_{31}}$$

If we compare this result with the derivation in reference [7] of the formula for determining the drift angle of a steady turning ship with zero rudder angle (see Fig.3), it has the form

$$\beta(0) = - \frac{q}{h_1 r_{31}}$$

It is easily observed that the value of the oscillation amplitude β_0 differs from the value of the drift angle in steady turning $\beta(0)$ by the linear harmonic coefficient term h_1^* . Otherwise the amplitude β_0 for towing an unstable ship for values $\bar{x}_t < 0.5$ are nearly the same as the value of drift angle of the ship (considered as self-propelled) in a steady turn for zero rudder angle (see Fig.5).

Having determined the amplitude, β_0 it is easy to estimate the frequency

$$\bar{v} = \bar{v} \frac{v}{L}$$

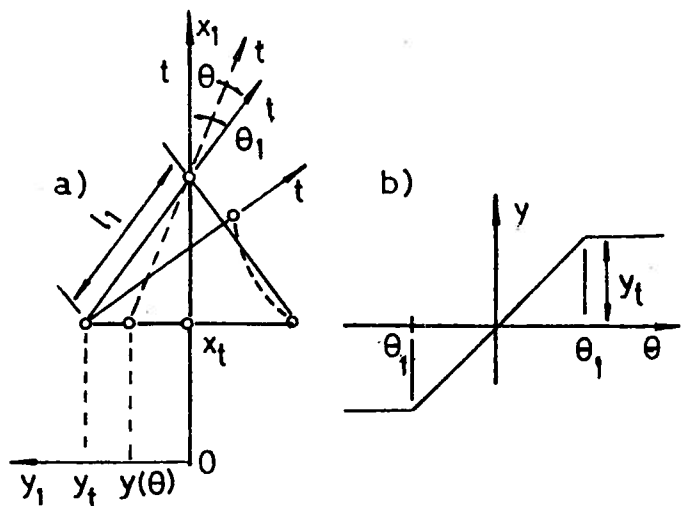


Figure 6 Diagram of harnessing bridle in towing (a) and dependence of ordinate Y on angle v

Here

$$\dot{v} = \frac{v}{L} \sqrt{\frac{\bar{s} + \bar{s}_{31} h_1^* \beta_0}{r_{31} + a_{21} + h_1^* \beta_0}}$$

This produced the systematic results in Figs. 4 and 5 which give the values for the drift angle β_p corresponding to states of stable and unstable equilibrium. These figures also give the amplitude of the drift angle in oscillatory behavior for the point where the towing cable is fastened for stable ($\bar{x}_{p\phi} > \bar{x}_\beta(0)$) and unstable ($\bar{x}_{p\phi} < \bar{x}_\beta(0)$) ships.

In conclusion it should be noted that it is perfectly fine to use a bridle during towing. The difference is that instead of the value of \bar{x}_t the value of \bar{x}_t^* is used when the towing bridle is adopted. It is defined as follows:

$$\bar{x}_t^* = \bar{x}_t + \ell_1$$

where ℓ_1 is related to the length of one leg of the towing bridle (Fig. 6).

To understand this relation consider the moment M_T and tow force T from the towing bridle relative to the ship's center of gravity.

$$M_t = x_t T \sin \theta + y T \cos \theta = T(x_t \theta + y)$$

For $y = y(\theta)$ where $y(\theta)$ is a nonlinear expression (Fig. 6-b)

In the limit $|\theta| < |\theta_1| y \doteq \ell_1 \theta$, this results in the following expression:

$$M_t = T(x_t + \ell_1) \theta = T \cdot x_t^* \theta$$

This corresponds to the case where the tow-rope attachment point is shifted forward along the vessel's centerplane.

LITERATURE

1. Collected Works of Academician A. N. Krylov, Vol. IX, No. 11, A.N. USSR, 1949.
2. Lavrentiev, V.M., "On the Tendency of Yawing and Maneuverability on Non-Propelled Ships," TRANSPORT, Leningrad, 1939.
3. Basin, A.M., "Course Stability and Maneuverability of Combined Tug and Barge," Report of Central Scientific Research Institute, 5, 1950.
4. Bogdanov, B.V., "On the Yawing of Ocean Barges," WATER TRANSPORT, Leningrad, 1953.
5. Vasilyev, A.V., "Investigation of Control Components," SYMPOSIUM ON SHIPBUILDING QUESTIONS, Gorky, GIIVI, 1969.
6. Bidel, S., "Yawing of Ships During Towing," Selected Articles from SHIPBUILDER AND MARINE ENGINEERING 70, No. 667, 1963.
7. Voitkunsky, A.I., Persiz, R.Y., Titov, I.A., HANDBOOK ON SHIP THEORY, Shipbuilding, Leningrad, 1973.



The University of Michigan is an equal opportunity/affirmative action employer. Under applicable federal and state laws, including Title IX of the Education Amendments of 1972, the University does not discriminate on the basis of sex, race, or other prohibited matters in employment, in educational programs and activities, or in admissions. Inquiries or complaints may be addressed to the University's Director of Affirmative Action and Title IX Compliance: Dr. Gwendolyn C. Baker, 5072 Administration Building, 763-0235.